Journal of Visualized Experiments

Measurement of 3-Dimensional cAMP Distributions in Living Cells Using 4-Dimensional (x, y, z, and λ) Hyperspectral FRET Imaging and Analysis

--Manuscript Draft--

Article Type:	Invited Methods Article - JoVE Produced Video
Manuscript Number:	JoVE61720R1
Full Title:	Measurement of 3-Dimensional cAMP Distributions in Living Cells Using 4-Dimensional (x, y, z, and λ) Hyperspectral FRET Imaging and Analysis
Corresponding Author:	Silas Josiah Leavesley, Ph.D. University of South Alabama Mobile, Alabama UNITED STATES
Corresponding Author's Institution:	University of South Alabama
Corresponding Author E-Mail:	leavesley@southalabama.edu
Order of Authors:	Naga S. Annamdevula
	Rachel Sweat
	Hayden Gunn
	John R. Griswold
	Andrea L. Britain
	Thomas C. Rich
	Silas Josiah Leavesley, Ph.D.
Additional Information:	
Question	**Response**
Please indicate whether this article will be Standard Access or Open Access.	Standard Access (US$2,400)
Please indicate the **city, state/province, and country** where this article will be **filmed**. Please do not use abbreviations.	Mobile, AL, USA
Please confirm that you have read and agree to the terms and conditions of the author license agreement that applies below:	I agree to the Author License Agreement
Please specify the section of the submitted manuscript.	Bioengineering
Please provide any comments to the journal here.	

Measurement of 3-Dimensional cAMP Distributions in Living Cells Using 4-Dimensional (x, y, z, and λ) Hyperspectral FRET Imaging and Analysis

Authors:
Naga S. Annamdevula[1, 2], Rachel Sweat[3], Hayden Gunn[1], John R. Griswold[3], Andrea L. Britain[1, 2], Thomas C. Rich[1, 2], Silas J. Leavesley[1, 2, 3]

[1]Department of Pharmacology, University of South Alabama, Mobile, AL, USA.
[2]Center for Lung Biology, University of South Alabama, Mobile, AL, USA.
[3]Department of Chemical and Biomolecular Engineering, University of South Alabama, Mobile, AL, USA.

Corresponding Author:
Silas J Leavesley
leavesley@southalabama.edu
Tel: (251) 460-6160

Email Addresses of Co-authors:
Naga S. Annamdevula (annamdevula.southalabama.edu)
Rachel Sweat (rachelsweat1@gmail.com)
Andrea Britain (abritain@southalabama.edu)
Hayden Gunn (ghg1621@jagmail.southalabama.edu)
John R. Griswold (jrg1522@jagmail.southalabama.edu)
Thomas Rich (trich@southalabama.edu)

Keywords: Cyclic AMP, spatial, FRET, hyperspectral, microscopy, spectral FRET.

Summary:
Due to inherent low signal-to-noise ratio (SNR) of Förster resonance energy transfer (FRET) based sensors, measurement of cAMP signals has been challenging, especially in three spatial dimensions. Here, we describe a hyperspectral FRET imaging and analysis methodology that allows measurement of cAMP distribution in three spatial dimensions.

Abstract:
Cyclic AMP is a second messenger that is involved in a wide range of cellular and physiological activities. Several studies suggest that cAMP signals are compartmentalized, and that compartmentalization contributes to signaling specificity within the cAMP signaling pathway. The development of Förster resonance energy transfer (FRET) based biosensors has furthered the ability to measure and visualize cAMP signals in cells. However, these measurements are often confined to two spatial dimensions, which may result in misinterpretation of data. To date, there have been only very limited measurements of cAMP signals in three spatial dimensions (x, y, and z), due to the technical limitations in using FRET sensors that inherently exhibit low signal to noise ratio (SNR). In addition, traditional filter-based imaging approaches are often ineffective for accurate measurement of cAMP signals in localized subcellular regions due to a range of factors,

including spectral crosstalk, limited signal strength, and autofluorescence. To overcome these limitations and allow FRET-based biosensors to be used with multiple fluorophores, we have developed hyperspectral FRET imaging and analysis approaches that provide spectral specificity for calculating FRET efficiencies and the ability to spectrally separate FRET signals from confounding autofluorescence and/or signals from additional fluorescent labels. Here, we present the methodology for implementing hyperspectral FRET imaging as well as the need to construct an appropriate spectral library that is neither undersampled nor oversampled to perform spectral unmixing. While we present this methodology for measurement of three-dimensional cAMP distributions in pulmonary microvascular endothelial cells (PMVECs), this methodology could be used to study spatial distributions of cAMP in a range of cell types.

Introduction:

Cyclic adenosine monophosphate (cAMP) is a second messenger involved in key cellular and physiological processes including cell division, calcium influx, gene transcription, and signal transduction. A growing body of evidence suggests the existence of cAMP compartments in the cell through which signaling specificity is achieved[1–7]. Until recently, cAMP compartmentalization was inferred based upon distinct physiological or cellular effects induced by different G-coupled receptor agonists[8–11]. More recently, FRET based fluorescence imaging probes have provided new approaches for the direct measurement and observation of cAMP signals in a cell[12–14].

Förster resonance energy transfer (FRET) is a physical phenomenon in which energy transfer occurs between donor and acceptor molecules in a non-radiative fashion when the molecules are in close proximity[15,16]. With the development of FRET based fluorescent indicators, this physical phenomenon has been used in biological applications to study protein-protein interactions[17], protein co-localization[18], Ca^{+2} signaling[19], gene expression[20], cell division[21] and cyclic nucleotide signaling. FRET based cAMP indicators typically consist of a cAMP binding domain, a donor fluorophore and an acceptor fluorophore[22]. For example, the H188 cAMP sensor[12,22] used in this methodology consists of a cAMP binding domain obtained from Epac, sandwiched between Turquoise (donor) and Venus (acceptor) fluorophores. At basal conditions (unbound), Turquoise and Venus are in an orientation such that FRET occurs between the fluorophores. Upon binding of cAMP to the binding domain, a conformational change occurs such that Turquoise and Venus move apart resulting in a decrease in FRET.

FRET based imaging approaches offer a promising tool for investigating and visualizing cAMP signals within a cell. However, current FRET based microscopic imaging techniques are often only partially successful in achieving sufficient signal strength to measure FRET with subcellular spatial clarity. This is due to several factors, including the limited signal strength of many FRET reporters, the high level of precision required to accurately quantify changes in FRET efficiency, and the presence of confounding factors, such as cellular autofluorescence[23,24]. The result is often a FRET image that is plagued by weak SNR, making visualization of subcellular changes in FRET very difficult. In addition, investigation of spatially localized cAMP signals has been almost exclusively performed in only two spatial dimensions and the axial cAMP distribution has been rarely considered[25]. This is likely because low SNR impeded the ability to measure and visualize cAMP gradients in three spatial dimensions. To overcome limitations of using FRET sensors with low

SNR, we have implemented hyperspectral imaging and analysis approaches to measure FRET in single cells[25–27].

Hyperspectral imaging approaches were developed by NASA to differentiate terrestrial objects present in satellite images[28,29]. These techniques have since been translated to the fluorescence microscopy field[30], with several commercial confocal microscope systems offering spectral detectors. In traditional (non-spectral) fluorescence imaging, the sample is excited using a band-pass filter or a laser line, and the emission is collected using a second band-pass filter, often selected to match the peak emission wavelength of the fluorophore(s). By contrast, hyperspectral imaging approaches seek to sample a complete spectral profile of either the fluorescence emission[26,31,32] or excitation[33,34] at specific wavelength intervals. In our previous studies, we showed that hyperspectral imaging and analysis approaches can offer improved quantification of FRET signals in cells when compared to traditional filter-based FRET imaging techniques[26]. Here, we present a methodology for performing 4-dimensional (x, y, z, and λ) hyperspectral FRET imaging and analysis to measure and visualize cAMP distributions in three spatial dimensions. These approaches have allowed visualization of agonist-induced cAMP spatial gradients in single cells[25]. Interestingly, depending on the agonist, cAMP gradients may be apparent in cells. The methodology presented here utilizes spectral unmixing of non-uniform background and cellular autofluorescence to improve the accuracy of the FRET measurements. While this methodology is demonstrated in pulmonary microvascular endothelial cells (PMVECs) using a cAMP FRET biosensor, the methodology could easily be modified for use with alternative FRET reporters or alternative cell lines.

Protocol:

This protocol follows procedures approved by the University of South Alabama Institutional Animal Care and Use Committee.

1. Cell, sample, and reagent preparation for imaging

1.1. Isolate rat pulmonary microvascular endothelial cells (PMVECs) as described previously[35].

NOTE: Cells were isolated and cultured by the Cell Culture Core at the University of South Alabama, Mobile, AL on 100 mm cell culture dishes.

1.2. Seed isolated PMVECs on 25 mm round glass coverslips and let them grow in the incubator at 37 °C until cells attain at least 80% confluency (at least 24 hours).

NOTE: Cells and cell type may vary from study to study and hence cell-specific cell culture procedures should be followed to seed and grow cells. The cell seeding and culturing protocol used in these studies is available as supplemental information in the file named “Supplemental File_Cell Culture and Transfection”.

1.3. Transfect PMVECs with a FRET biosensor and incubate for 48 hours at 37 °C.

NOTE: Protocol to transfect PMVECs is also described in the supplemental information file named "Supplemental File_Cell Culture and Transfection".

1.4. On the day of imaging, warm Tyrode's buffer to 37 °C in a water bath.

NOTE: Tyrode's buffer consists of 145 mM NaCl, 4 mM KCl, 10 mM HEPES, 10 mM Glucose, 1 mM $MgCl_2$ and 1 mM $CaCl_2$

1.5. Mount a coverslip containing transfected cells into a cell chamber and secure the top with a mounting gasket to prevent leaking.

1.6. Wipe the bottom of the coverslip using a delicate task wipe to clean any excess media or adherent cells.

1.7. Add 800 µL of working buffer and 4 µL of 5 mM nuclear label to the cell chamber and gently rock for 5 – 10 seconds.

NOTE: When adding buffer or reagent solutions to coverslips mounted in the cell chamber, make sure to add the solution gently and at the side of the cell chamber so as not to dislodge adherent cells. Adding 4 µL of 5 mM nuclear label to 800 µL of buffer makes 25 µM final concentration of nuclear label. For loosely adherent cells such as HEK293 cells, mix nuclear label and buffer in a vial first and then add to coverslips mounted in the cell chamber. This will prevent lifting the cells off the coverslip.

1.8. Cover the cell chamber with aluminum foil to protect from light and incubate for 10 minutes at room temperature.

1.9. Reagent Preparation: Add 1 µL of 50 mM forskolin to 199 µL of buffer. This will produce a final concentration of forskolin of 50 µM when added to cells that were prepared with 800 µL of buffer. 1 µL of DMSO in 199 µL of buffer should also be prepared to be used as a vehicle control.

NOTE: In these studies, forskolin is used as an adenylyl cyclase activator to stimulate cAMP production. If desired, this methodology can easily be modified to allow treatment with alternative reagents for stimulating or inhibiting adenylyl cyclase, phosphodiesterases, etc.

2. Image acquisition

2.1. Use a confocal microscope equipped with a spectral detector.

NOTE: All image acquisition steps outlined here were developed using a commercially available Nikon A1R microscope system. These steps may need to be adjusted if using an alternative spectral microscope. Ensure that all equipment is turned on at least 30 minutes prior to the start of the experiment so as to reach stable operating conditions.

2.2. Select the 60x water immersion objective and add a drop of water to the objective.

NOTE: For high-resolution live-cell imaging, it is recommended to use a high numerical aperture objective. Please refer to the List of Materials for information about the objective used in these studies.

2.3. Place the loaded cell chamber (from step 1.7) onto the microscope stage.

2.4. Select the DFT (DAPI/FITC/TRITC) filter set by tuning the filter knob on the right side of the microscope.

2.5. Operate the microscope in fluorescence widefield mode using the eyepieces to select a field of view containing cells expressing the cAMP FRET sensor.

NOTE: Ensure that the average intensity of the FRET signal at the donor or acceptor emission peak wavelength in the selected cell is at least 100 intensity units (A.U.) or at least 4X the baseline signal of a region with no expressing cells. This can be confirmed using the spectrum profile viewer available in NIS Elements software. When looking for a cell with good signal, it is advisable to discard excessively bright cells (they may be compromised).

2.6. Open NIS software, switch to confocal mode, unlock the laser interlock button and click on **Live**.

2.7. Use the focus knob to focus on the cells by looking at the preview on the screen.

2.8. Configurate device, acquisition, and z-stack settings in the software, as described below.

2.9. Acquisition settings:

NOTE: Camera and device acquisition settings can be applied using a previously acquired image. Open the image, right click and select **Reuse Camera Settings**.

2.9.1. Open the A1 settings menu, check the boxes corresponding to 405 nm and 561 nm laser lines, select **SD** for spectral detections, select 10 for resolution and 31 for channels.

NOTE: A1 settings menu is shown as a small gear icon on the top left corner of the A1 Plus Settings window. 405 nm laser is used for donor excitation and 561 nm laser is used for nuclear label excitation.

2.9.2. Set the wavelength range (410 – 730 nm) by selecting start and end wavelength values.

2.9.3. Click the binning/skip icon in the A1 settings menu and select the box that is numbered 15, then click **OK** on the A1 settings menu.

NOTE: This is to remove the wavelength channel that corresponds to the 561 nm excitation laser (this is typically the 15th wavelength channel). It is important not to use this wavelength band to avoid an artificially low signal, which can create a spectral artifact. The signal is lower in this band because of the mechanical finger that covers the detector element to protect it from laser damage.

2.9.4. Set the laser intensities to 8% and 2% for the 405 nm and 561 nm lasers, respectively, Si Hv (detector gain) at 149, and a pinhole radius of 2.4 airy disk units.

NOTE: Laser intensities may have to be adjusted depending on the age of the instrument and condition of the lasers. If adjusting laser intensities between different samples or experimental groups, it is important to maintain the same ratio of laser intensities (e.g., 8:2). In addition, it is important to select a laser intensity that is not so bright as to create rapid photobleaching. Gain should be adjusted to maximize signal intensity while minimizing detector noise. For these studies, a gain of 149 was used. A pinhole size of 2.4 AU was selected as a balance between acquiring images with sufficient signal to noise ratio (SNR) and maintaining optical sectioning (confocality). An increase in pinhole size increases SNR but decreases confocality.

2.9.5. Set the scan speed to 0.25 spectral frames per second, select the icon corresponding to unidirectional for scan direction, enter 4 for the count, and set 1024 x 1024 for scan size.

NOTE: FRET signals are weak, and a slow scan speed is often required. Using scan speed of 0.25, acquisition of a spectral z-stack is completed in ~3 minutes. Scan speed can be increased or decreased depending on the fluorophores used. For example, for brighter fluorophores like eGFP, faster scan speed (2 fames/second) can be used. The number entered under count corresponds to a frame averaging value of 4, which helps in noise reduction during image acquisition. For very stable samples and where time is not a constraint, higher averaging values (up to 16) can be used to obtain images with improved SNR.

2.10. Define z-stack acquisition parameters:

NOTE: The values entered in steps 2.10 may need to be adjusted to accommodate changes in fluorescent label binding or concentration, type of label, number of labels used, cell line, and other changes in sample preparation that may affect cell labeling density and/or cellular autofluorescence. When adjusting acquisition parameters, care should be taken to achieve a sufficient SNR while minimizing photobleaching. In addition, when configuring a spectral FRET assay, care should be taken to ensure that parameters work well across all treatment groups. It is advisable to run a trial of each treatment group with the proposed parameter settings to ensure that SNR is sufficient and photobleaching is minimized.

2.10.1. Open the ND acquisition window by clicking **view → acquisition control → ND acquisition**.

2.10.2. Enter the path/destination and a file name to save the ND file on the popup window.

2.10.3. Check the box corresponding to **z-series**.

2.10.4. Click on **live** in the A1 Plus Settings window. This will open a live viewing window.

2.10.5. Adjust the focus knob on the microscope to select the top of the cell and click **Top** in the ND acquisition window to set the current position as the top.

NOTE: It is suggested to focus slightly above the top of the cell to ensure that all of the cell is sampled in the z series.

2.10.6. Adjust the focus knob on the microscope to select the bottom of the of the cell and click on **Bottom** in the ND acquisition window to set the current position as the bottom.

NOTE: Focus slightly below the bottom of the cell to ensure that all of the cell is sampled.

2.10.7. Enter 1 µm for step size, select top-bottom for the z-scan direction and click **run** on the ND Acquisition window to acquire a z-stack.

NOTE: Step size determines the number of z-slices that will be acquired depending on top and bottom locations (i.e., the distance traveled). A 1 µm step size was selected as a compromise between imaging speed, z-axis sampling, and photobleaching. Using the confocal pinhole diameter of 2.4 AU and the 60x water immersion objective resulted in optical section thickness of 1.73 µm. Hence, a 1 µm step size is slightly below the Nyquist sampling criteria, but this is a compromise that was made to reduce the time needed to acquire a z-stack. For very stable samples, for which speed is not critical, a smaller z-axis step and possibly a smaller confocal pinhole diameter may be used to increase z-axis resolution. Bottom-top should yield similar results and can be used to evaluate any effects of photobleaching that may occur during the z scan.

2.11. Set up the Perfect Focus System (PFS) if available:

NOTE: PFS allows the system to compensate for fluctuations in the focal depth during image acquisition. The following steps may be used to set up PFS, and these steps may vary slightly depending on the version of the Nikon A1R and the version of NIS Elements used.

2.11.1. Highlight symmetric mode defined by the range icon in the ND acquisition window.

2.11.2. Turn on the PFS button on the front face of the microscope (make sure the dichroic mirror knob located on the section below the sample stage is ‘in’).

2.11.3. Redefine the top (rotate counterclockwise) and bottom (rotate clockwise) using the knob on the front face of the PFS offset controller.

2.11.4. Define a relative z-position/z-depth by clicking 'relative' on the ND acquisition window.

2.11.5. Click memory on the front face of the microscope so that the software memorizes the relative z-depth.

2.12. After the z-stack acquisition is complete, gently add the desired reagent (forskolin or vehicle control) using a pipette and wait for 10 minutes.

NOTE: Add the reagent very gently so as not to disturb the cells or move the position of the cell chamber within the microscope XY stage; it is helpful to verify in a subsequent live view or image that the field of view has not shifted during reagent addition. The 10-minute wait time is for the forskolin treatment to take effect. If an alternative treatment is used, the wait time may need to be adjusted.

2.13. After 10 minutes, change the filename and click **run** in the ND acquisition window.

2.14. Repeat steps 2.11 – 2.13 as outlined above for at least 5 coverslips so as to achieve sufficient results for statistical analysis (n=5 for each treatment group – forskolin and vehicle control).

2.15. Prepare samples and sample blanks to construct the spectral library and acquire spectral images using similar acquisition settings as outlines in steps 2.9 and 2.10.

3. Image analysis

NOTE: These images will be used to construct a spectral library containing the pure spectra of all individual endmembers present in the study. The endmembers in the spectral library might vary from study to study if different fluorophores are used. A detailed procedure to construct the spectral library is provided in a supplemental information file named "Supplemental File_Spectral Library". Exporting data to .tiff files, linear spectral unmixing, FRET efficiency measurements, three-dimensional reconstruction, and cAMP levels estimation. Image analysis can be performed using different image analysis and programming platforms such as ImageJ, Python, MATLAB, or CellProfiler. In these studies, MATLAB scripts were used.

3.1. Export image data:

3.1.1. Create new folders with the same filename corresponding to the spectral z-stack images acquired in steps 2.13 and 2.14.

NOTE: The following steps outlined to export data are specific for NIS Elements AR version 4.30.01. These steps may vary slightly depending on the version of the software.

3.1.2. Click **File**, which will open a File Window. Browse and select the spectral image file acquired in step 2.12 and click **Open**.

3.1.3. Once the file loads, click **File→ Import/Export→ Export ND document**.

3.1.4. On the popup window: browse and select the folder created in step 3.1.1, select Tagged Image Format (TIF) for File type, then select **Mono image for each channel** and **Keep bit depth**.

NOTE: The File prefix will be pre-generated; change this value for convenience. The Index order will change depending on the Channels that are selected, and should display "z, c" for indexing according to z-slice location first and wavelength band number second. Make sure that the boxes corresponding to **Apply LUTs** or **Insert Overlays** or **Use Point Names** are unselected.

3.1.5. Click **Export** to export the tiff files to a destination folder as individual tiff files.

3.1.6. Repeat steps 3.1.2 – 3.1.5 to export spectral image files acquired in step 2.13.

3.2. Linear spectral unmixing:

3.2.1. Open the programming software.

NOTE: Custom developed programming script to unmix raw spectral images is provided on the University of South Alabama BioImaging and BioSystems website, under the Resources tab (https://www.southalabama.edu/centers/bioimaging/resources.html).

3.2.2. Open the file labeled "Linear Unmixing.m" and click the **run** button in the editor toolbar.

3.2.3. Browse and select the folder containing the exported *.tif file sequence generated by the NIS Elements software.

3.2.4. Click **OK** to continue, which will open a new window called **Wavelength and Z-Slice**.

3.2.5. Copy the filename of first file (without z-slice and channel number) in the folder selected in step 3.2.4 and paste it into the first step of the dialog box labeled "Enter the Image Name".

3.2.6. Enter the number of channels in the second step labeled "Enter the number of wavelength bands", number of z-slices in the third step labeled "Enter the number of Z-slices" and click **OK**.

NOTE: The number of wavelengths bands may change if changes are made to the acquisition settings, such as adjusting the wavelength range or the wavelength step size. The number of Z-slices may also change depending on the height of the cell.

3.2.7. Browse and select the wavelength file called "Wavelength.mat" in the popup window labeled "Select the wavelength information file" and click **open**.

3.2.8. Browse and select the "Library.mat" file in the new popup window labeled "Select the spectral library file", click **open** and wait until the unmixing of the slices is finished.

NOTE: Library.mat file is a file containing pure spectra for each endmember fluorophore along with cell autofluorescence and background spectral signatures. In this case, endmember fluorophores include Turquoise, Venus, and DRAQ5. Background spectral signatures include cellular or matrix autofluorescence, coverslip fluorescence, and coverslip diffraction. Wavelength.mat file is a file containing wavelength channel information used to acquire the spectral image. An example library file and wavelength file are available on Bioimaging and Biosystems website (see the note under 3.2.1). For more information on how to generate spectral library and wavelength files, refer to supplemental information file named "Supplemental File_Spectral Library". Unmixed images corresponding each z-slice will be saved into the folder called "Unmixed" created during the unmixing process within the folder that was selected in step 3.2.3.

3.3. FRET Efficiency Calculation:

3.3.1. Open the programing script called "multiFRRCF.m" and click **run**.

NOTE: This programming file is available from the University of South Alabama Bioimaging and Biosystems website (see note under step 3.2.1).

3.3.2. Enter the number of experimental trials to analyze in the popup dialogue box called "how many folders to reslice" and click **OK**.

NOTE: Image data from each experiment should be saved in a separate unmixed image folder. This step simply allows the analysis code to loop over many folders as a time saving step.

3.3.3. Browse and select the unmixed folder(s) and click **OK**.

NOTE: The number of times that the "Browse for folder" pop up window opens depends on the number entered in "How many folders to reslice" dialogue box in the previous step. Browse and select the folders one after the other.

3.3.4. On the new popup window, enter the following information into the respective boxes: **scaling factor** is 12.4, **Threshold** is 5.6, **X**, **Y**, **and Z Frequency** are 5, 5, and 1 respectively, and **smoothing algorithm** is Gaussian.

NOTE: The scaling factor is a value in pixels/µm and will be used to scale the Z-direction sampling to that of the XY direction. The scaling factor is obtained from the image pixel size, which is usually provided as metadata in the image for most confocal microscope systems. For example, if the image is acquired with 0.08 µm/pixel spacing, the scaling factor should be 12.5 pixels/µm. Threshold value will be used to threshold the images and generate a binary mask of the cell. We

created a list of optimum values based on the image donor+acceptor intensity. Use 4.5 as a thresholding value if the image has bright donor+acceptor intensity and low background, a value between 5.6 to 6.5 for images having only moderate donor+acceptor intensity and/or higher background, and a value of 7.5 and above for images having a donor+acceptor intensity that is lower than the background. Frequency value corresponds to the frequency in number of pixels at which the slicing is performed in the subsequent steps. For example, if the Z-depth of the cell is 17 µm with a 1 µm step size and a scaling factor of 12.5 pixels/µm is used in the XY direction, then the depth of the 3-dimensional image dataset will be resampled at 212 pixels (Z direction). Based on the Z frequency value entered (for example, 1 pixel), the 3-dimensional image data set will be re-sliced beginning at the top of the image data set and then moving in increments of 1 pixel downward. This results in 212 resliced images. If a larger frequency value were entered for Z Frequency, then fewer resliced images would be generated. Resliced images are saved in subsequent steps.

3.3.5. Click **run** and wait until all the FRET measurements and reslicing are performed.

NOTE: A separate folder is created within the parent directory to which resliced grayscale FRET efficiency images and colored (a colormap applied) FRET efficiency images are saved. For example, all grayscale and colormap FRET images resliced in the X direction (YZ plane) are saved into a folder called "Resliced_XFRET".

3.3.6. Repeat the analysis with similar settings for all the experiments – before and after forskolin treatments and vehicle controls.

NOTE: Steps mentioned in section 3.3 describe the values to enter for the custom FRET analysis programming script to generate 3-dimensional FRET image data. However, this script executes several operations while running, including: loading image data, creating image stacks, smoothing, FRET efficiency calculations, creating and applying a cell border mask, 3-dimensional image reconstruction, reslicing 3-dimensional images at specified intervals (frequencies), applying a colormap for visualizing FRET changes, and saving the resliced image data to the same directory. Additional details have been included as comments in the program script.

4. Mapping FRET efficiency to cAMP levels

4.1. Open the programming file named 'Mapping_FRET Efficiency_to_cAMP_concentration.m' and click **run** on the main window.

NOTE: The file is available on the BioImaging and BioSystems website (see note under 3.2.1). This file reads grayscale FRET efficiency images and converts them to a cAMP levels based on a characteristic curve. This characteristic curve uses a cAMP-to-FRET relationship documented in literature[15,36] that is described by the Hill equation (equation shown in Table 1). However, K_d of the probe in intact cells is difficult to estimate and we have assumed it to be 1 µM in our calculations. Hence, results are shown as a function of K_d. (i.e., [cAMP] = x* K_d). Equations used to measure FRET efficiency and mapping FRET to cAMP levels are shown below:

$$E = \frac{a_{apparent} - d_{apparent}}{a_{apparent} + d_{apparent} * \frac{Q_a}{Q_d} * k^{\lambda}}$$

Where E is FRET efficiency, $a_{apparent}$ and $d_{apparent}$ are unmixed pixel intensities of acceptor and donor images, respectively.
Q_a and Q_d are quantum yields of acceptor and donor. Q_a and Q_d cancel out when the equation for k^{λ} is incorporated in the FRET efficiency equation, k^{λ} is a correction factor:

$$k^{\lambda} = \frac{\varepsilon_d^{\lambda} Q_d}{\varepsilon_a^{\lambda} Q_a}$$

ε_d^i and ε_a^i are extinction coefficients of donor and acceptor at the donor excitation wavelength, *i* (405nm).

$$[cAMP] = \left(\frac{E}{1-E}\right) K_D$$

E is FRET efficiency and K_D = Dissociation constant = 1.

4.2. Navigate and select the first grey scale FRET image (saved in step 3.3.5) and click OK.

4.3. Open the FRET/cAMP images to inspect the distribution of cAMP signals in three dimensions.

Representative Results:

This protocol describes the use of hyperspectral FRET imaging and analysis approaches to measure cAMP gradients in three spatial dimensions in living cells. There are several key steps involved in generating these results, for which careful attention is required while analyzing and quantifying the data. These key steps include construction of an appropriate spectral library, background spectral unmixing, thresholding to identify cell borders, and FRET efficiency calculations. **Figure 1** illustrates the schematic flow of all the steps involved in measuring FRET efficiency and cAMP levels in living cells. When performed properly, these imaging and analysis steps will allow measurement of FRET efficiency and estimation of cAMP spatial gradients in 3 dimensions in a cell, while accounting for non-uniform background signals.

Figure 2 depicts 3-dimensional views of false-colored raw hyperspectral image data acquired using a Nikon A1R confocal microscope at baseline conditions (

Figure 2A) and 10 minutes after (

Figure 2B) forskolin treatment. Note that similar detector and system parameters were used to acquire before and after treatment image stacks to maintain consistency for quantitative

519 analysis. Also note that changes in FRET are not obvious in this image, as this is purely a
520 visualization of raw data, before calculating the FRET efficiency.
521
522 A spectral library with pure spectra of all end members is needed to further analyze raw
523 spectral image data. Constructing an appropriate spectral library is one of the key steps to
524 ensure appropriate measurements of FRET efficiency.

525 **Figure 3** demonstrates the construction of a spectral library containing the pure spectra of
526 endmembers (in these current studies, the endmembers are Turquoise, Venus, and DRAQ5). To
527 measure FRET efficiency, it is important to obtain the spectra of Turquoise and Venus using a
528 sample with 1:1 stoichiometry. Here, we have provided an approach where the acceptor
529 fluorophore is completely photo-destructed, allowing spectral signatures of the donor and
530 acceptor with 1:1 stoichiometry to be obtained (

531 **Figure 3A-F**). In addition, linear power relationships among the lasers (

532 **Supplemental Figure 1**) were applied to calculate the acceptor spectrum with an intensity that
533 would be expected if it were excited using the donor excitation laser, in this case 405 nm for
534 Turquoise (

535 **Figure 3G**). This ensures that unmixed donor and acceptor signals are comparable in absolute
536 intensity when FRET is excited with a single 405 nm laser line. Non-transfected cells labeled
537 with the nuclear dye, DRAQ5 (

538 **Figure 3H**) were utilized to obtain the pure spectrum of DRAQ5 (

539 **Figure 3I**). Combining the spectra of the donor, Turquoise (

540 **Figure 3F**), acceptor, Venus (

541 **Figure 3G**), and DRAQ5 (

542 **Figure 3I**), a 3-component library was created (

543 **Figure 3J**).
544
545 Signals from sources other than the fluorescent labels may also be present in a sample. To
546 account for these, three different spectral signatures with peaks that occur at 424 nm, 504 nm,
547 and 574 nm were identified within unlabeled cellular samples. We believe that these spectral
548 signatures correspond to coverslip reflectance and cell matrix or cellular autofluorescence.

549 **Figure 4** depicts the sources of these three background spectral signatures. It is important to note
550 that these signals are distributed non-uniformly within the sample and hence cannot simply be
551 subtracted out. However, adding the spectral signatures of these signals to the spectral library
552 and using linear unmixing to separate the signals presents an approach for removing these
553 confounding signals from the donor and acceptor signals prior to calculating FRET efficiencies. To
554 achieve this, the three background spectral signatures were added to the 3-component spectral

library, forming a new 6-component library consisting of donor (Turquoise), acceptor (Venus), DRAQ5 and three background spectral signatures.

A custom programming script was written to unmix the spectral image data into individual endmembers, and a separate script was written to perform subsequent FRET efficiency calculations. Linear spectral unmixing (illustrated in

Figure 5) was performed using the 6-component spectral library. Unmixing was performed for each slice in the axial image stack, also referred to as z-stack (refer to the 3-dimensional visualization of raw spectral image data in

Figure 5A). This resulted in separate unmixed images for each endmember, for each z-slice in the z-stack (

Figure 5C – E, background unmixed images are not shown). If desired, the unmixed signals may be false-colored for visualization with a different color assigned to each unmixed signal (

Figure 5F-H).

Figure 6 illustrates the steps involved in the FRET efficiency calculations, as well as the steps for mapping FRET efficiency to cAMP levels. A FRET efficiency image was generated using smoothed unmixed donor and acceptor images. A binary mask image was obtained using unmixed donor, acceptor, and nuclear images. The mask was applied to the FRET efficiency image to remove contributions from pixels outside of the cell. Though unmixed images from single z-slices were used for the pictorial demonstration of FRET efficiency measurements, these calculations were performed on each slice within the 3-dimensional image stack. The 3-dimensional FRET image data set was then resliced in three orthogonal planes to visualize spatial gradients of cAMP signals in different directions.

Visualizing agonist-induced changes in FRET efficiency and cAMP levels

The steps described above provide a method for calculating FRET efficiency and cAMP levels from hyperspectral image data in three spatial dimensions. These steps can be applied to cellular preparations before and after treatment with compounds that elicit a cAMP response, such as forskolin. Here, we provide an example of using this approach to observe changes in FRET and cAMP distribution in PMVECs following treatment with 50 μM forskolin.

Figure 7 illustrates the changes in FRET efficiency and cAMP levels in different XY plane slices (z slices), from apical to basal, allowing comparison of baseline conditions (before forskolin treatment) and 10-minutes post-treatment. In this illustrative example, FRET efficiency decreased (columns 1 and 2 in

Figure 7) upon forskolin treatment, correlating to an increase in cAMP levels (columns 3 and 4 in

Figure 7). Minimal spatial variation of cAMP within a single XY plane was observed. However, axial (apical-to-basal) cAMP spatial gradients were observed, as can be surmised by noting that the apical slice has a deeper red color (indicating higher cAMP levels through the color lookup table that was applied) than the basal slice after forskolin treatment (column 4 in

Figure 7). Axial FRET or cAMP distributions can often be better visualized using images obtained from the two orthogonal spatial planes:

Figure 8 depicts the FRET efficiency and cAMP levels in the YZ plane at baseline (columns 1 and 2) and 10 minutes after forskolin treatment (columns 3 and 4), while
Supplemental Figure 2 depicts the FRET efficiency and cAMP level changes in the XZ plane. These results demonstrate the feasibility of measuring FRET and estimating cAMP levels from 3-dimensional hyperspectral image data and also demonstrate the importance of visualizing axial distributions of FRET or cAMP. While beyond the scope of this methodological paper, it may be that axial spatial distributions of cyclic nucleotides contribute to specificity within cyclic nucleotide signaling pathways.

When performing the methods described above, it is important to meticulously check the accuracy of the steps and to run appropriate experimental and vehicle controls to ensure that changes in FRET (and corresponding cAMP) are due to actual changes in donor and acceptor signals and are not imaging artifacts. For example, important steps to consider include:

Using an appropriate spectral library that contains all of the needed spectral components
As mentioned, there can be significant contribution of background signals from cellular autofluorescence, deposited matrix, or reflected light from the coverslip (excitation-emission bleed through).

Figure 9 represents an example data set illustrating that the background signal was retained within the images when a 3-component (Turquoise, Venus, and DRAQ5) library was used to unmix the spectral data. By contrast, the background signal was effectively removed when a more complete (and appropriate) 6-component spectral library was used.

Using an optimal threshold value to generate a cell mask
In many of the experiments that we have performed, the background signal intensity is approximately 50-60% of the FRET signal intensity that is present within the raw spectral image data (i.e., when visualizing unprocessed spectral image data the peak of the FRET signal is only ~2X higher than that of the surrounding background signal). Thus, separation of background signal from foreground signal using a threshold value to obtain a binary mask is a sensitive step and must be carefully performed in order to avoid analysis artifacts.

Figure 10 illustrates the effect of different threshold values applied for cell segmentation to create a binary mask of the cell. A low threshold value may include background signal as part of the expressing cell. On other hand, an overly high threshold value may preclude measurement of FRET in low-expressing cells or regions of a cell with low donor+acceptor signal (either very

thin portions of the cell or portions that may have a lower regional concentration of the FRET probe).

Selecting a transfected cell with donor+acceptor signal intensity ≥ background signal

Figure 11 illustrates an example data set where FRET efficiencies and corresponding levels were measured from unmixed images obtained using a 6-component spectral library for linear spectral unmixing. Despite using the 6-component library to unmix spectral image data and selecting a high threshold for creating the cell border and nuclear mask, FRET efficiency images were still prone to high background noise signal near the basal side of the cell. In this case, the presence of background noise was due to selection of a cell that was only weakly expressing the FRET probe, and the donor+acceptor signal strength was approximately equal to the background signal strength, even after unmixing. Thus, in addition to applying the sophisticated analysis steps described above, it is also important to select a cell with sufficient expression of the FRET probe and correspondingly sufficient FRET signal (donor and acceptor signal at least equal or above the noise signal) during acquisition in order to ensure high-quality results.

FIGURE LEGENDS:

Figure 1: Flowchart depicting the steps involved in FRET efficiency and level measurements in three spatial dimensions using hyperspectral FRET imaging and analysis.

Figure 2. **A 3-dimensional visualization of a cell expressing the cAMP FRET reporter (green) and nuclei from the cell and surrounding non-expressing cells (red).** Raw spectral image data acquired using a Nikon A1R spectral confocal microscope have been false colored according to wavelength and visualized in 3 dimensions using NIS Elements software. A) 3-dimensional image data at baseline and B) 10 minutes after 50 µM forskolin treatment.

Figure 3. **Construction of a spectral library containing the pure spectra of fluorescent labels in the study (referred to as endmembers by the remote sensing field).** A) A false-colored image of cells expressing the FRET biosensor acquired at 405 nm excitation (donor excitation). B) Spectrum corresponding to FRET signal: 4 different regions of interest (ROIs) were drawn on image A shown by red, yellow, blue and green rectangles. Average intensity at each wavelength for each ROI selected was exported. The average intensity from these 4 ROIs was plotted at each emission wavelength. The emission peaks of the spectrum correspond to both the donor (Turquoise) and the acceptor (Venus) fluorophores. C) A false-colored image of cells expressing the FRET biosensor acquired at 488 nm excitation (acceptor excitation). D) The average spectrum was estimated as explained in B from several ROIs in C (the same regions as in A) with emission peak due only to the acceptor. E) A false-colored image of cells expressing the FRET biosensor acquired at 405 nm excitation after photo-destruction of the acceptor fluorophore by 514 nm irradiation. F) The average spectrum was estimated as explained in B from several ROIs in E (the same regions as A) with emission peak due only to the donor. NOTE that the donor intensity is increased in F when compared to that of the original FRET signal, indicating that after photobleaching of the acceptor, donor excitation is leading to direct donor emission. G) The acceptor spectrum as would

be expected if obtained using 405 nm excitation. This was estimated by utilizing the facts that the 405 nm and 488 nm excitation lasers have a linear response which can be characterized using a spectrometer and integrating sphere (
Supplemental Figure 1) and the wavelength-dependent extinction coefficient of Venus. Hence, the Venus spectrum obtained at 488 nm excitation can be converted into the Venus spectrum that would be expected if obtained at 405 nm excitation H) A false-colored image of cells labeled with the nuclear label, DRAQ5. I) The average spectrum from several regions of interest in H. J) The resultant spectral library containing the normalized pure spectra of the donor and DRAQ5 and the excitation wavelength–corrected spectrum of the acceptor. Note that Turquoise and Venus spectra were normalized to the maximum value of combined Turquoise + Venus spectral data while DRAQ5 was simply normalized to unity at the value of the peak emission wavelength.

Figure 4: Background spectral signatures were identified and included into the spectral library to account for background fluorescence signals during the unmixing process. A, B) Two background fluorescence spectral signatures were observed when characterizing a sample blank (unlabeled coverslip). These spectral signatures were named based on their peak wavelengths – one at 424 nm (from coverslip fluorescence) and the other at 504 nm (likely from reflectance or back scatter). C) A third background spectral signature was observed with a peak emission wavelength of 574 nm when non-labeled cells were analyzed, potentially from cellular autofluorescence or fluorescence of the underlying matrix. D) Background spectra extracted from images A, B, and C. These three background spectra were added to the existing 3-component library (
Figure 3J) to develop a 6-component spectral library.

Figure 5: Linear spectral unmixing using a 6-component spectral library that accounts for background signals. A) Raw spectral image data acquired as an axial z-stack. B) 6-component spectral library used to linearly unmix raw spectral data. C, D, and E) Gray scale unmixed images of DRAQ5, Turquoise, and Venus, respectively, resulted from linear spectral unmixing. F, G, and H) False colored unmixed images of DRAQ5, Turquoise, and Venus respectively. Unmixed images of background signals were also calculated (data not shown here as only the fluorescent labels are of interest for this methodology – refer to Figure 4 in Annamdevula, et al. for examples of unmixed background signals[25]).

Figure 6: Flowchart depicting the steps involved in calculating FRET and cAMP levels from unmixed spectral image data. A) Representative unmixed image of donor, Turquoise. B) Representative unmixed image of acceptor, Venus. C) Representative unmixed image of nuclei, DRAQ5. D) Binary cell mask is generated by thresholding unmixed donor+acceptor summed image. E) A threshold is applied to the nuclear image to create a binary mask of the nucleus. F) The pixel wise FRET efficiency was calculated from unmixed donor and acceptor images. G) A composite binary mask was created from cell border and nuclear masks. H) Masked FRET efficiency image: composite cell mask was applied to FRET efficiency image to exclude non-specific FRET signals outside the cell and within the nucleus. I) A colormap was applied to the masked FRET efficiency image to better visualize spatial changes in FRET. J) The cAMP levels image that was estimated from the FRET efficiency image. K) Colormap was applied to better

visualize spatial changes in cAMP. Colorbars shown on the right side were used to visualize FRET efficiency (top panel) and cAMP levels (bottom panel). Images shown in this figure are representative of one single axial z-slice, but the analysis operation described in this figure is performed on the entire axial z-stack.

Figure 7: Forskolin-induced FRET efficiency and cAMP spatial gradients visualized in PMVECs. XY plane images were generated by reslicing 3-dimensional reconstructed FRET and cAMP image data in the axial (Z) direction from the apical to the basal side of the cell. Five contiguous XY slices are shown. Columns 1 and 3 represent the FRET efficiency at baseline and 10 minutes after treatment with 50 µM forskolin, respectively. Columns 2 and 4 indicate the levels at baseline and 10 minutes after forskolin treatment. The colorbars were used to relate changes in the colormap to FRET efficiency (top) and cAMP levels (bottom). White lines shown on images in column 2 and column 4 are used to generate the intensity profile (line scan profile) of cAMP signals across this selected line. Intensity profile plot obtained from the mid-slice of the cell at baseline (blue profile) and after forskolin treatment (green profile) demonstrates the spatial distribution of cAMP signals across the line scan. Scale bar indicates 20 µm.

Figure 8: Forskolin-induced FRET efficiency and cAMP spatial gradients visualized in the axial direction. YZ plane images were generated by reslicing 3-dimensional reconstructed FRET and cAMP image data in the lateral (X) direction (from left to right side of the cell). Columns 1 and 3 represent the FRET efficiency at baseline and at 10 minutes after 50 µM forskolin treatment, respectively. Columns 2 and 4 represent the cAMP levels at baseline and at 10 minutes after forskolin treatment. The colorbars at right were used to relate changes in the colormap to FRET efficiency (top) and cAMP levels (bottom).

Figure 9: A comparison of the effectiveness of utilizing either a 3-component or a 6-component spectral library for calculating FRET and cAMP levels images. Nonspecific background signals were observed in images calculated using a 3-component library, which did not account for background spectral signatures. This was especially true for images near the basal side of the cell following 50 µM forskolin treatment (column 2). By contrast, background signal artifacts were effectively removed when using a 6-component library that included background spectral signatures, improving the ability to segment the cell and analyze FRET and cAMP signals.

Figure 10: Image analysis artifacts can be introduced if an appropriate threshold value is not selected to delineate the cell and nuclear borders. Unmixed donor and acceptor images were used to create a mask with three different threshold values: 0.35 (columns 1 as 2), 0.65 (columns 3 and 4) and 0.9 (columns 5 and 6). Columns 1, 3, and 5 display the FRET efficiency at baseline. Columns 2, 4, and 6 display the FRET efficiency at 10 minutes after 50 µM forskolin treatment. Selecting a threshold that was too low resulted in portions of the background, or extracellular region, being included with the cell for analysis, while selecting a threshold that is too high resulted in the loss of part of the cell (see the apical slice in columns 4-5 when compared to columns 3-4).

Figure 11: Background signal artifacts may still persist even after background unmixing and selecting an appropriate threshold during creation of a binary mask. Column 1 shows representative apical, middle, and basal slices at baseline and column 2 shows the same at 10 minutes after 50 µM forskolin treatment. Despite using a 6-component library for unmixing that accounted for background signals and utilizing a higher threshold of 0.85 for binary mask generation, background regions were still identified as being part of the cell, especially after treatment with forskolin. If this occurs, a possible explanation may be that a cell with weak expression of the FRET reporter was selected for imaging.

Supplemental Figure 1: Measurements of laser line intensity as a function of laser setting in the software. A fiber-coupled spectrometer and integrating sphere were calibrated to a NIST-traceable lamp to measure laser intensity for both the 405 nm laser line and the 488 nm laser line. A) Total number of photons measured at the microscope stage corresponding to different laser intensities of the 405 nm laser. B) Total number of photons measured at the microscope stage corresponding to different laser intensities of 488 nm laser. Linear response in laser intensity was observed for both the lasers as measured at the microscope stage. A linear trendline was fit and the trendline equation for each laser line was used to calculate the acceptor spectrum that would be expected if excited with the 405nm laser line (donor excitation).

Supplemental Figure 2: Forskolin-induced FRET efficiency and cAMP spatial gradients visualized in the axial direction. XZ plane images were generated by reslicing 3-dimensional reconstructed FRET and cAMP image data in the lateral (Y) direction (from front to back of the cell). Columns 1 and 3 represent the FRET efficiency at baseline and at 10 minutes after 50 µM forskolin treatment, respectively. Columns 2 and 4 represent the cAMP levels at baseline and at 10 minutes after forskolin treatment. The color bars at right were used to relate changes in the colormap to FRET efficiency (top) and cAMP levels (bottom). Similar to results shown for the YZ planes (

Figure 8), apical to basal spatial gradients in FRET efficiency and cAMP levels may be visualized as changes in color from the top to bottom of a single YZ slice, both at baseline conditions (any given slice in columns 1-2) and after 50 µM forskolin treatment (columns 3-4).

DISCUSSION:

The development of FRET biosensors has allowed the measurement and visualization of cyclic nucleotide signals in single cells, and there is great promise for visualizing subcellular signaling events[13,22,37,38]. However, the use of FRET biosensors presents several limitations, including the low signal-to-noise characteristics of many fluorescent protein-based FRET reporters and the weak transfection or expression efficiencies of the FRET reporters (this may be especially challenging in certain cell lines, such as PMVECs)[23,24]. Imaging of weakly expressed fluorescent proteins, combined with ratiometric FRET calculations, often results in a high degree of uncertainty or fluctuation in the calculated FRET efficiency. In an effort to improve the reliability of FRET measurements, we and others have previously demonstrated the use of hyperspectral imaging and analysis to measure FRET signals and to reduce crosstalk or bleed through of fluorescence signals between fluorescent labels and autofluorescence effects[26,31,32,39]. Due to

limitations in signal strength, these spectral FRET studies were limited to two (X and Y) spatial dimensions until very recently. Hence, they provided a single-slice view of FRET changes within a cell.

In recent studies, we noted that FRET (and corresponding cAMP levels) appeared to be spatially distributed not just in the XY plane, but also across the XZ and YZ planes[25]. The hyperspectral FRET imaging approach described here extends our ability to visualize and measure FRET and cyclic nucleotide (cAMP) changes into three spatial dimensions, opening new possibilities for assessing signal compartmentalization. This 4-dimensional (X, Y, Z, and λ) hyperspectral imaging and analysis approach allows the measurement and visualization of cAMP gradients in three spatial dimensions while accounting for non-uniform background signals. Here, we have demonstrated how to implement this approach through the example of forskolin-induced cAMP spatial gradients. In the post-treatment image data, cAMP spatial gradients can be observed from the apical to the basal side of the cell (

Figure 7 and

Figure 8). The cAMP produced upon treatment with forskolin did not appear to reach cell-cell junctions (

Figure 7 and

Figure 8).

In utilizing the methodology described here, it was important to account for different sources of background and autofluorescence signals to allow accurate estimation of FRET efficiencies. Linear unmixing provides a potential avenue for accounting for unique background spectra, if their signatures are different than the fluorescent probes of interest. In particular, linear unmixing is better suited for separating background and autofluorescence signals than standard background subtraction.[40–42] In the example shown here, three different spectral signatures were measured and assigned a name based on the peak emission wavelength of the signature: the 424 nm background spectrum (possibly from the coverslip fluorescence), the 504 nm background spectrum (likely due to reflected or back-scattered light), and the 574 nm background spectrum (possibly due to cell or cellular matrix autofluorescence). To illustrate the effects of failing to account for these signatures, two spectral libraries were created, and unmixed images compared. First, a spectral library containing just the fluorescent labels in the sample, Turquoise, Venus, and DRAQ5, was created and labeled the 3-component library. Second, a spectral library that additionally contained the three background spectral signatures was created and labeled the 6-component library. As shown above, unmixing with the 6-component library (background unmixing) allowed removal of background signals, whereas unmixing with the 3-component library did not (

Figure 9). In previous work, we have shown that the root mean squared error (RMSE) associated with linear unmixing is decreased when using a spectral library that accounts for both the

fluorescent labels and background signatures. It should be noted that the axial distribution of background fluorescence is often non-uniform and hence, a simple background subtraction will not work to correct the image data. Thus, the spectral unmixing approach is needed to provide accurate background removal and reliable FRET measurements.

It is important to optimize system parameters to select the best possible system and camera settings when acquiring spectral images. The overall goal should be to optimize SNR while minimizing acquisition time and preventing photobleaching.[43] Thus, when optimizing an imaging system, a compromise between spatial, temporal, and spectral resolutions is often needed. In these studies, optimal values were selected for the system and camera settings including pinhole size, laser power, scan speed, scan size, and frame averaging as described in the protocol section. Utilizing these settings, the spatial sampling of 80 nm/pixel, temporal sampling of ~3 minutes per spectral z-stack (~10 seconds/XY image) and spectral sampling of 10 nm interval is achieved with negligible or minimal photobleaching.

To ensure accurate estimates of FRET efficiency, it is necessary to measure donor and acceptor spectra as they would be expected with 1:1 stoichiometry and identical excitation wavelengths (

Figure 3). Turquoise and Venus spectra were normalized with respect to the Turquoise peak emission wavelength. The FRET efficiency that was estimated using this spectral library produced values similar to those reported in literature[12,22]. Typically, endmember spectra in the library are normalized to unity. However, to accurately calculate FRET efficiency, the acceptor spectrum must be acquired with respect to the donor spectrum (i.e., at equimolar concentration or 1:1 stoichiometry and referenced to the same excitation wavelength). In addition to the use of a properly constructed library, several steps are involved in appropriate estimation of FRET efficiency and avoidance of analysis artifacts. These include selecting an expressing cell with adequate signal intensity (

Figure 11), smoothing of unmixed images before estimating FRET efficiency (Gaussian blur was applied in this example), using an appropriate threshold value to create the mask (

Figure 10), and estimation of a correction factor using extinction coefficients of donor and acceptor (**Table 1**). When these steps are followed, 3-dimensional distributions of FRET efficiency and underlying cAMP levels can be accurately visualized in single cells.

Localized cAMP signals have been estimated in 2-spatial dimensions using targeted FRET biosensors[13,37]. However, targeting FRET probes to specific subcellular compartments (for example, plasma membrane or lipid rafts) typically results in an increased local concentration of probe. This may result in measurement artifacts introduced due to intermolecular or bimolecular FRET. In addition, the results presented here and in Annamdevula et.al., 2018, Cytometry A[25] demonstrate the importance of 3-dimensional measurements of FRET from either soluble or targeted probes.

Despite the importance of measuring cAMP signals in three spatial dimensions, there are also limitations to this approach. The most restrictive limitation is the long acquisition times required – approximately 3 minutes per spectral z-stack. This acquisition rate precludes using this approach for detecting anything other than quasi – steady state cAMP distributions in cells. That said, the results presented demonstrate the importance of including quasi – steady state 3-dimensional (x, y, z) cAMP measurements as critical complements to standard 2-dimensional (x, y) measurements. In the future it will be interesting to incorporate labeled proteins and cellular structures into the experimental design. Careful choice of fluorophores used to label proteins (and/or structures) would allow assessment of the 3-dimensional distributions of the labeled proteins and FRET without additional loss of acquisition speed. This would in turn allow measurement of localized cAMP signals and cAMP signals near the labeled proteins in three spatial dimensions, thus offering an important experimental complement to targeted cAMP probes and further expanding the utility of hyperspectral measurements of 3-dimensional cAMP distributions in living cells.

ACKNOWLEDGEMENTS:

The authors would like to acknowledge Dr. Kees Jalink (The Netherlands Cancer Institute and van Leeuwenhoek Center for Advanced Microscopy, Amsterdam, the Netherlands) for providing us with the H188 cAMP FRET biosensor and Kenny Trinh (College of Engineering, University of South Alabama) for technical help in reducing the time taken to run our custom developed programming scripts.

The authors would like to acknowledge the funding sources: American Heart Association (16PRE27130004), National Science Foundation; (1725937) NIH, S100D020149, S10RR027535, R01HL058506, P01HL066299).

DISCLOSURES:

Drs. Leavesley and Rich disclose financial interest in a start-up company, SpectraCyte, LLC, that was formed to commercialize spectral imaging technologies. However, all procedures described in this protocol were conducted using commercially available products not associated with SpectraCyte, LLC.

REFERENCES:

1. Corbin, J. D., Sugden, P. H., Lincoln, T. M., Keely, S. L. Compartmentalization of adenosine 3':5'-monophosphate and adenosine 3':5'-monophosphate-dependent protein kinase in heart tissue. *The Journal of Biological Chemistry.* **252**, 3854–3861 (1977).
2. Terrin, A. et al. PGE1 stimulation of HEK293 cells generates multiple contiguous domains with different [cAMP]: role of compartmentalized phosphodiesterases. *The Journal of Cell Biology.* **175**, 441–451 (2006).
3. Bacskai, B. J. et al. Spatially resolved dynamics of cAMP and protein kinase A subunits in Aplysia sensory neurons. *Science.* **260**, 222–226 (1993).
4. Iancu, R. V., Ramamurthy, G., Harvey, R. D. Spatial and temporal aspects of cAMP signalling in cardiac myocytes. *Clinical and Experimental Pharmacology & Physiology.* **35**, 1343–1348 (2008).

5. Brunton, L. L., Hayes, J. S., Mayer, S. E. Functional compartmentation of cyclic AMP and protein kinase in heart. *Advances in Cyclic Nucleotide Research.* **14**, 391–397 (1981).
6. Hohl, C. M., Li, Q. Compartmentation of cAMP in adult canine ventricular myocytes. Relation to single-cell free Ca2+ transients. *Circulation Research.* **69**, 1369–1379 (1991).
7. Rich, T. C. et al. A uniform extracellular stimulus triggers distinct cAMP signals in different compartments of a simple cell. *Proceedings of the National Academy of Sciences of the United States of America.* **98**, 13049–13054 (2001).
8. Sayner, S. L., Alexeyev, M., Dessauer, C. W., Stevens, T. Soluble adenylyl cyclase reveals the significance of cAMP compartmentation on pulmonary microvascular endothelial cell barrier. *Circulation Research.* **98**, 675–681 (2006).
9. Rich, T. C., Tse, T. E., Rohan, J. G., Schaack, J., Karpen, J. W. In vivo assessment of local phosphodiesterase activity using tailored cyclic nucleotide–gated channels as cAMP sensors. *The Journal of General Physiology.* **118**, 63–78 (2001).
10. Blackman, B. E. et al. PDE4D and PDE4B function in distinct subcellular compartments in mouse embryonic fibroblasts. *Journal of Biological Chemistry.* **286**, 12590–12601 (2011).
11. Sayner, S. L. et al. Paradoxical cAMP-induced lung endothelial hyperpermeability revealed by Pseudomonas aeruginosa ExoY. *Circulation Research.* **95**, 196–203 (2004).
12. Klarenbeek, J., Jalink, K. Detecting cAMP with an EPAC-based FRET sensor in single living cells. *Methods in Molecular Biology.* **1071**, 49–58 (2014).
13. Surdo, N. C. et al. FRET biosensor uncovers cAMP nano-domains at β-adrenergic targets that dictate precise tuning of cardiac contractility. *Nature Communications.* **8**, 15031 (2017).
14. Ponsioen, B. et al. Detecting cAMP-induced Epac activation by fluorescence resonance energy transfer: Epac as a novel cAMP indicator. *EMBO Reports.* **5**, 1176–1180 (2004).
15. Vogel, S. S., Thaler, C., Koushik, S. V. Fanciful FRET. *Science's STKE* **2006**, re2 (2006).
16. Clegg, R. M. The History of FRET: From conception through the labors of birth. Reviews in Fluorescence, Vol. 3 (2006).
17. Giepmans, B. N. G., Adams, S. R., Ellisman, M. H., Tsien, R. Y. The fluorescent toolbox for assessing protein location and function. *Science.* **312**, 217–224 (2006).
18. Manzella-Lapeira, J., Brzostowski, J. A. Imaging protein-protein interactions by Förster resonance energy transfer (FRET) microscopy in live cells. *Current Protocols in Protein Science.* **93**, e58 (2018).
19. Cooper, D. M. F., Mons, N., Karpen, J. W. Adenylyl cyclases and the interaction between calcium and cAMP signalling. *Nature.* **374**, 421–424 (1995).
20. Sassone-Corsi, P. Coupling gene expression to cAMP signalling: role of CREB and CREM. *The International Journal of Biochemistry & Cell Biology.* **30**, 27–38 (1998).
21. Rebhun, L. I. Cyclic nucleotides, calcium, and cell division. *International Review of Cytology.* **49**, 1–54 (1977).
22. Klarenbeek, J., Goedhart, J., Van Batenburg, A., Groenewald, D., Jalink, K. Fourth-generation Epac-based FRET sensors for cAMP feature exceptional brightness, photostability and dynamic range: characterization of dedicated sensors for FLIM, for ratiometry and with high affinity. *PLOS ONE.* **10**, e0122513 (2015).
23. Leavesley, S. J., Rich, T. C. FRET: signals hidden within the noise. *Cytometry Part A.* **85**, 918–920 (2014).

24. Rich, T. C., Webb, K. J., Leavesley, S. J. Can we decipher the information content contained within cyclic nucleotide signals? *The Journal of General Physiology.* **143**, 17–27 (2014).
25. Annamdevula, N. S. et al. Spectral imaging of FRET-based sensors reveals sustained cAMP gradients in three spatial dimensions. *Cytometry Part A.* **93(10)**, 1029–1038. (2018).
26. Leavesley, S. J., Britain, A. L., Cichon, L. K., Nikolaev, V. O., Rich, T. C. Assessing FRET using spectral techniques. *Cytometry Part A.* **83**, 898–912 (2013).
27. Leavesley, S. J., Rich, T. C. Overcoming limitations of FRET measurements. *Cytometry Part A* **89**, 325–327 (2016).
28. Fink, D. J. Monitoring Earcths Resources from Space. *Technology Review.* **75**, 32–41 (1973).
29. Goetz, A. F. H., Vane, G., Solomon, J. E., Rock, B. N. Imaging Spectrometry for Earth Remote Sensing. *Science.* **228**, 1147–1153 (1985).
30. Bücherl, C. A., Bader, A., Westphal, A. H., Laptenok, S. P., Borst, J. W. FRET-FLIM applications in plant systems. *Protoplasma.* **251**, 383–394 (2014).
31. Chen, Y., Mauldin, J. P., Day, R. N., Periasamy, A. Characterization of spectral FRET imaging microscopy for monitoring nuclear protein interactions. *Journal of Microscopy.* **228**, 139–152 (2007).
32. Zimmermann, T., Rietdorf, J., Girod, A., Georget, V., Pepperkok, R. Spectral imaging and linear un-mixing enables improved FRET efficiency with a novel GFP2–YFP FRET pair. *FEBS Letters.* **531**, 245–249 (2002).
33. Griswold, J. R., Annamdevula, N., Deal, J., Rich, T., Leavesley, S. Estimating FRET Efficiency using Excitation-Scanning Hyperspectral Imaging. *Biophysical Journal.* **112**, 586a (2017).
34. Favreau, P. F. et al. Excitation-scanning hyperspectral imaging microscope. *Journal of Biomedical Optics.* **19**, 046010 (2014).
35. King, J. et al. Structural and functional characteristics of lung macro- and microvascular endothelial cell phenotypes. *Microvascular Research.* **67**, 139–151 (2004).
36. Thaler, C., Koushik, S. V., Blank, P. S., Vogel, S. S. Quantitative multiphoton spectral imaging and its use for measuring resonance energy transfer. *Biophysical Journal.* **89**, 2736–2749 (2005).
37. Agarwal, S. R. et al. Compartmentalized cAMP signaling associated with lipid raft and non-raft membrane domains in adult ventricular myocytes. *Frontiers in Pharmacology.* **9**, 332 (2018).
38. Johnstone, T. B., Agarwal, S. R., Harvey, R. D., Ostrom, R. S. cAMP signaling compartmentation: Adenylyl cyclases as anchors of dynamic signaling complexes. *Mol Pharmacol* mol.117.110825 (2017). doi:10.1124/mol.117.110825
39. Zhang, J., Li, H., Chai, L., Zhang, L., Qu, J., Chen, T. Quantitative FRET measurement using emission-spectral unmixing with independent excitation crosstalk correction. *Journal of Microscopy.* **257**, 104–116 (2015).
40. Zhang, J., Lin, F., Chai, L., Wei, L., Chen, T. IIem-spFRET: improved Iem-spFRET method for robust FRET measurement. *Journal of Biomedical Optics.* **21**, 105003 (2016).
41. Levy, S. et al. SpRET: highly sensitive and reliable spectral measurement of absolute FRET efficiency. *Microscopy and Microanalysis.* **17**, 176–190 (2011).
42. West, S. J. et al. Hyperspectral Measurements Allow Separation of FRET Signals from Non-Uniform Background Fluorescence. *Biophysical Journal*. **112**, 453a (2017).
43. Annamdevula, N. S. et al. An approach for characterizing and comparing hyperspectral microscopy systems. *Sensors (Basel).* **13**, 9267–9293 (2013).

1017

Figure 1

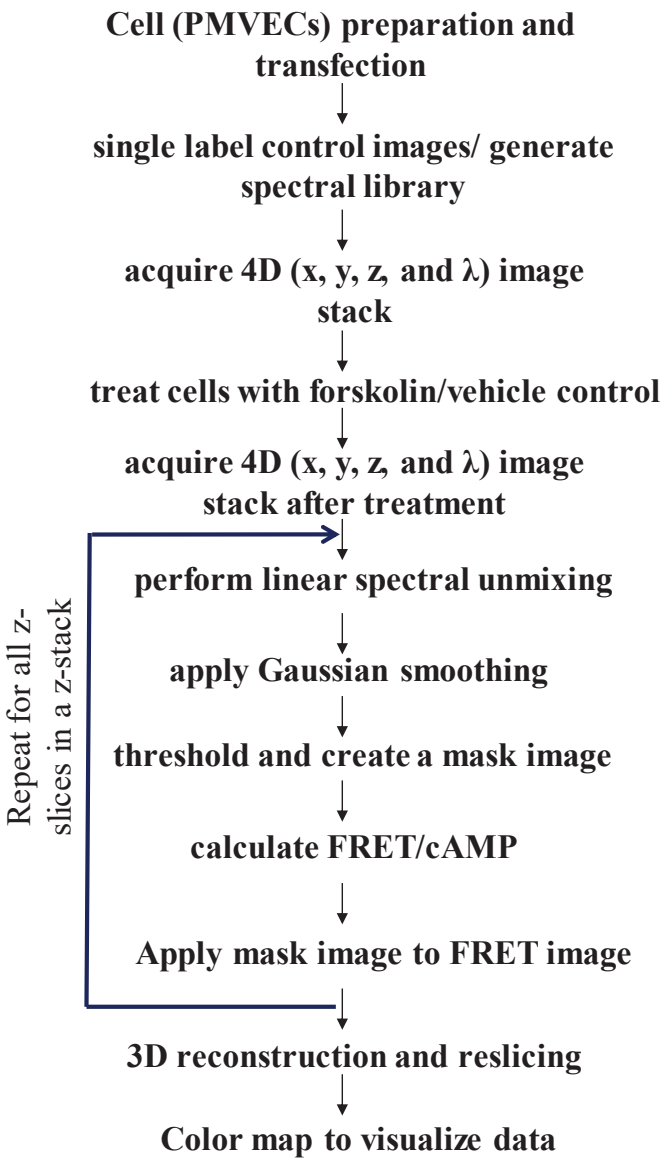

Figure 2

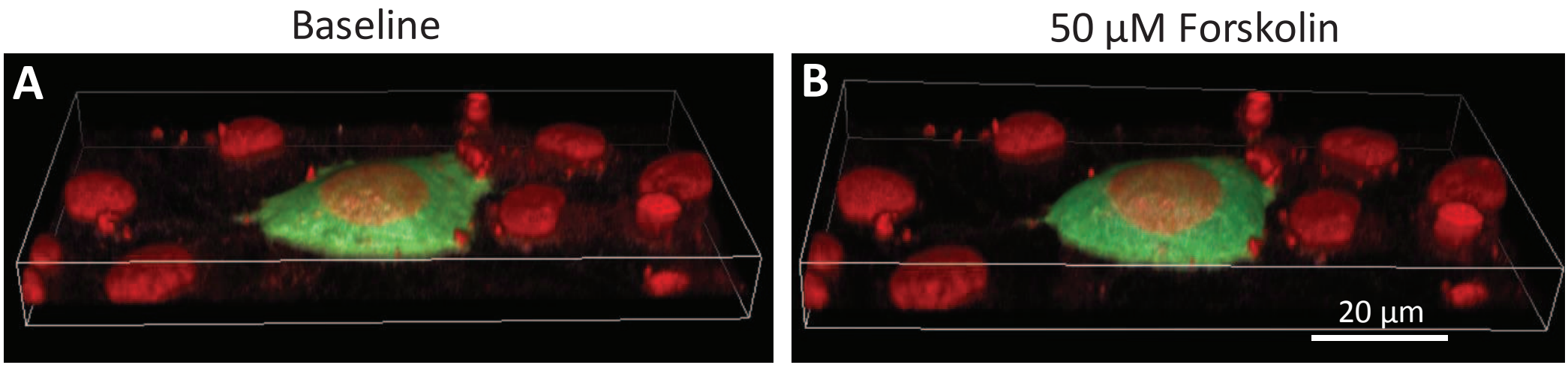

Figure 3

Click here to access/download;Figure;Figure 3.eps

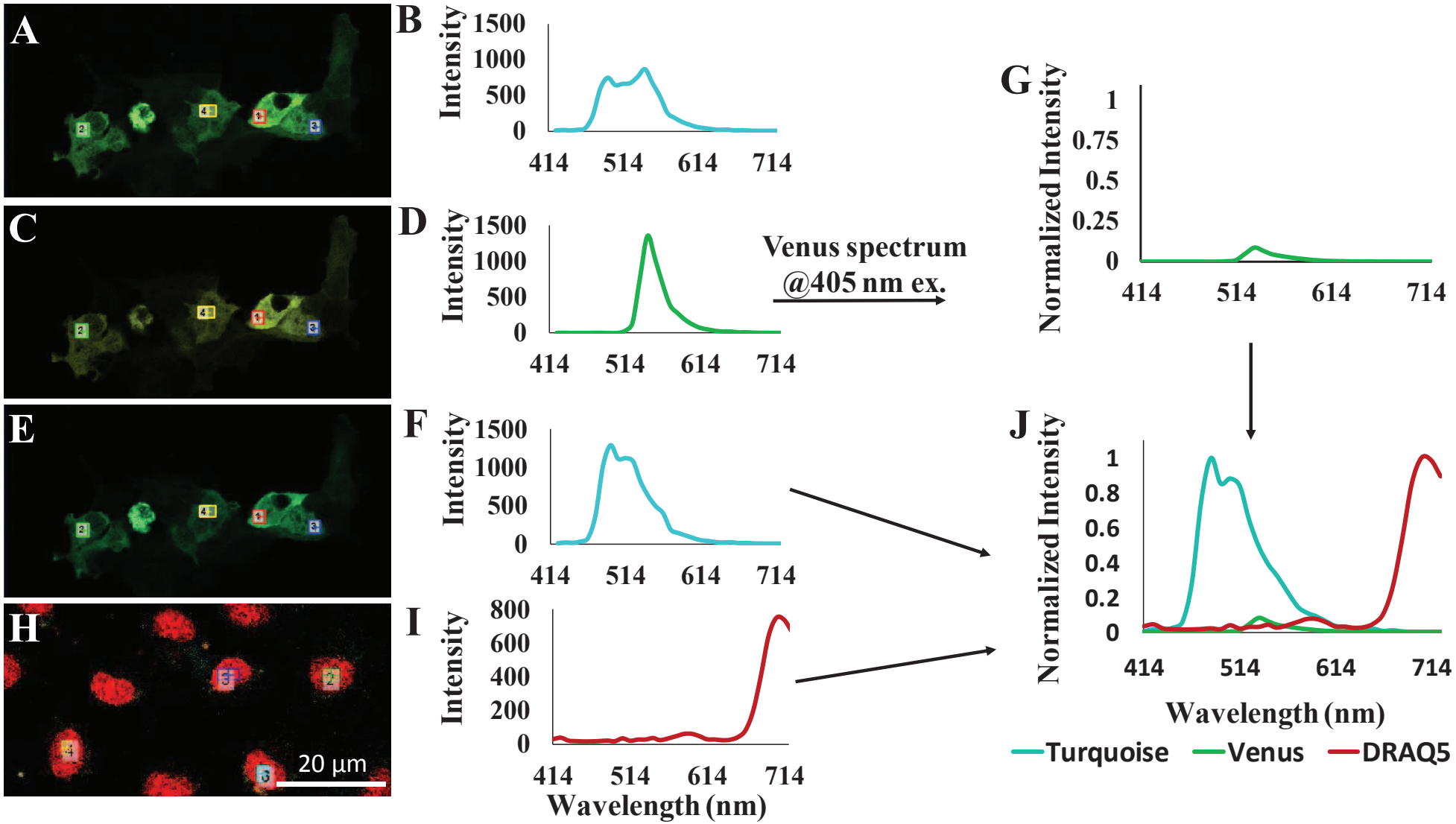

Figure 4

Click here to access/download;Figure;Figure 4.eps

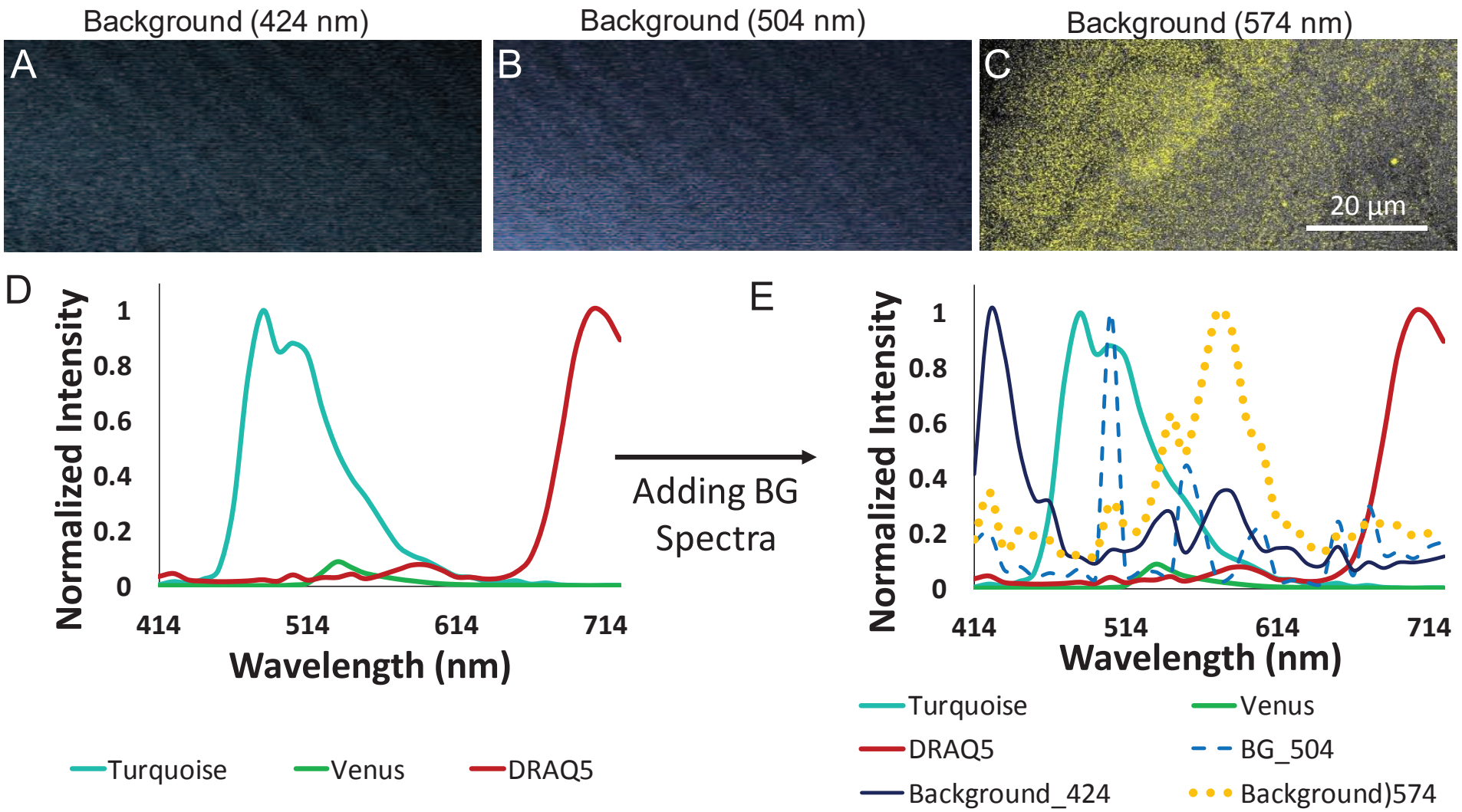

Figure 5

Click here to access/download;Figure;Figure 5.eps

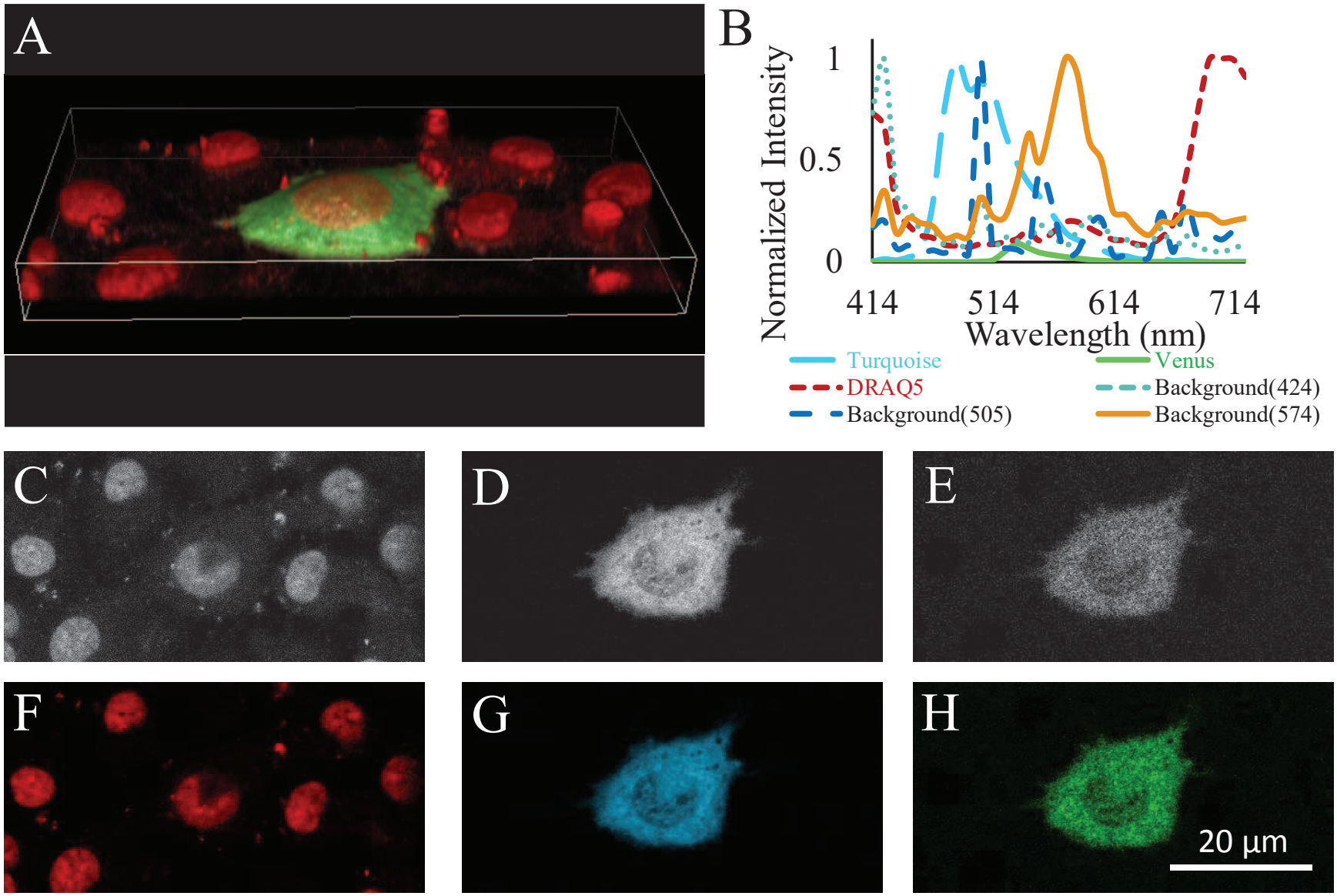

Figure 6

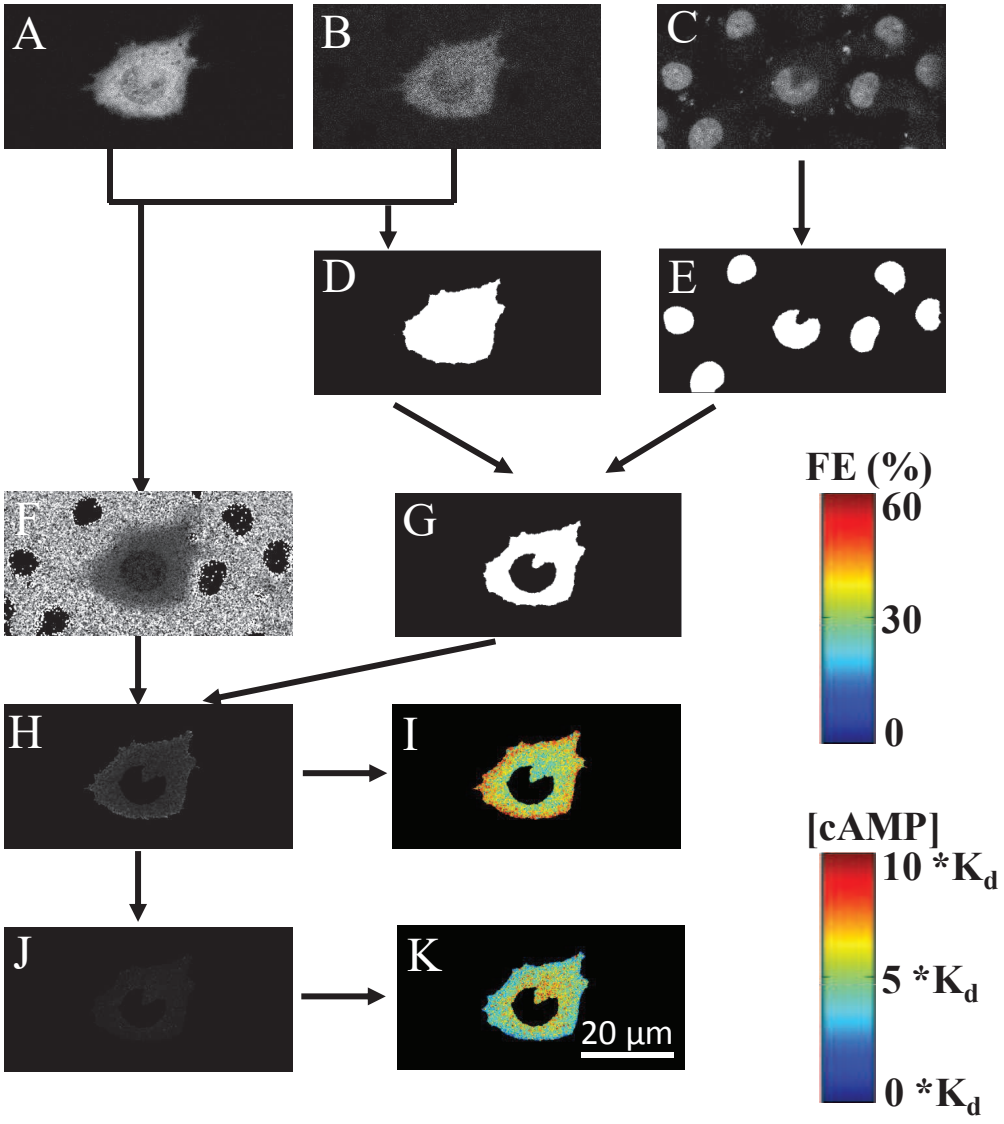

Figure 7

Click here to access/download;Figure;Figure 7.eps

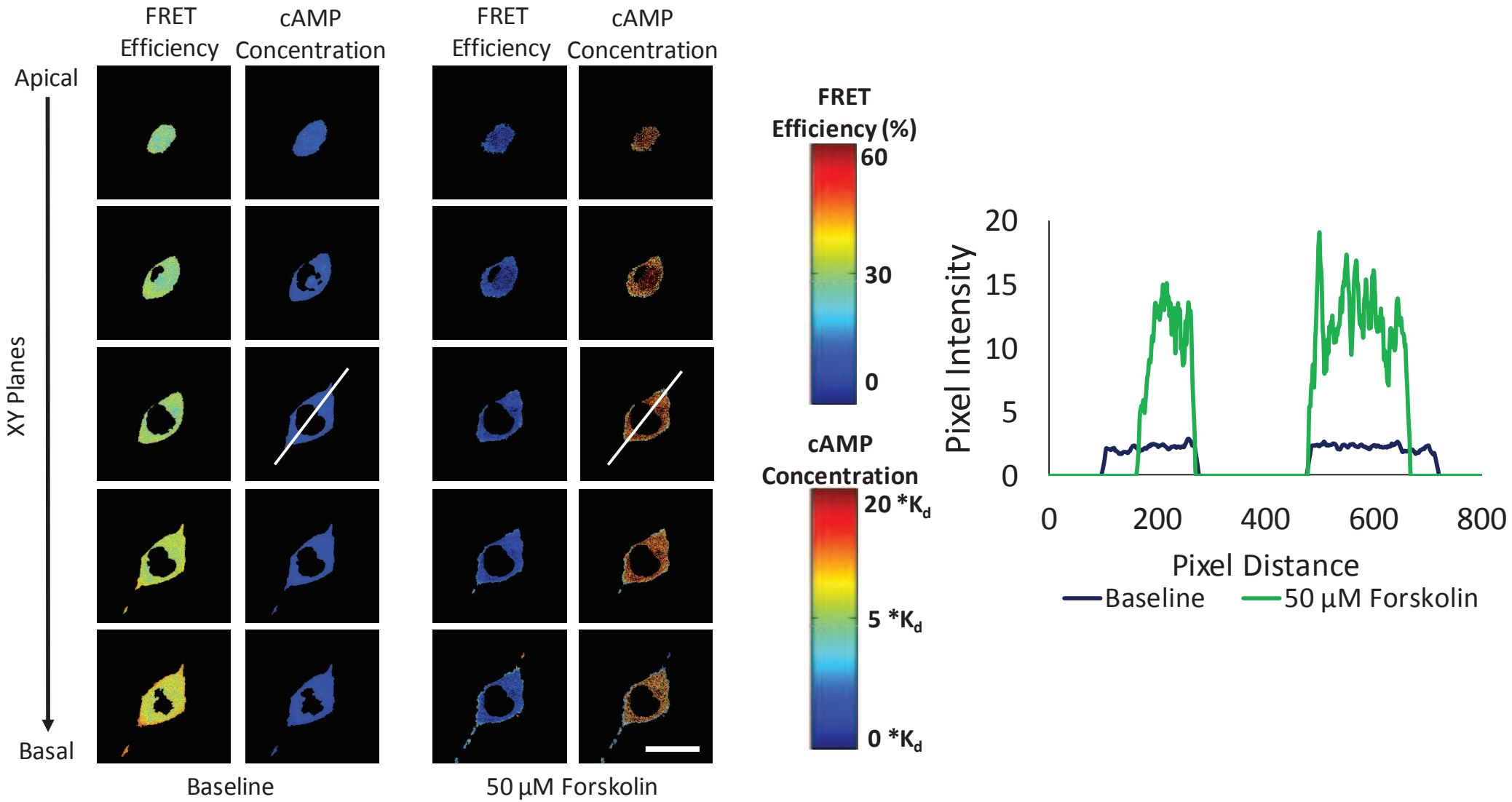

Figure 8

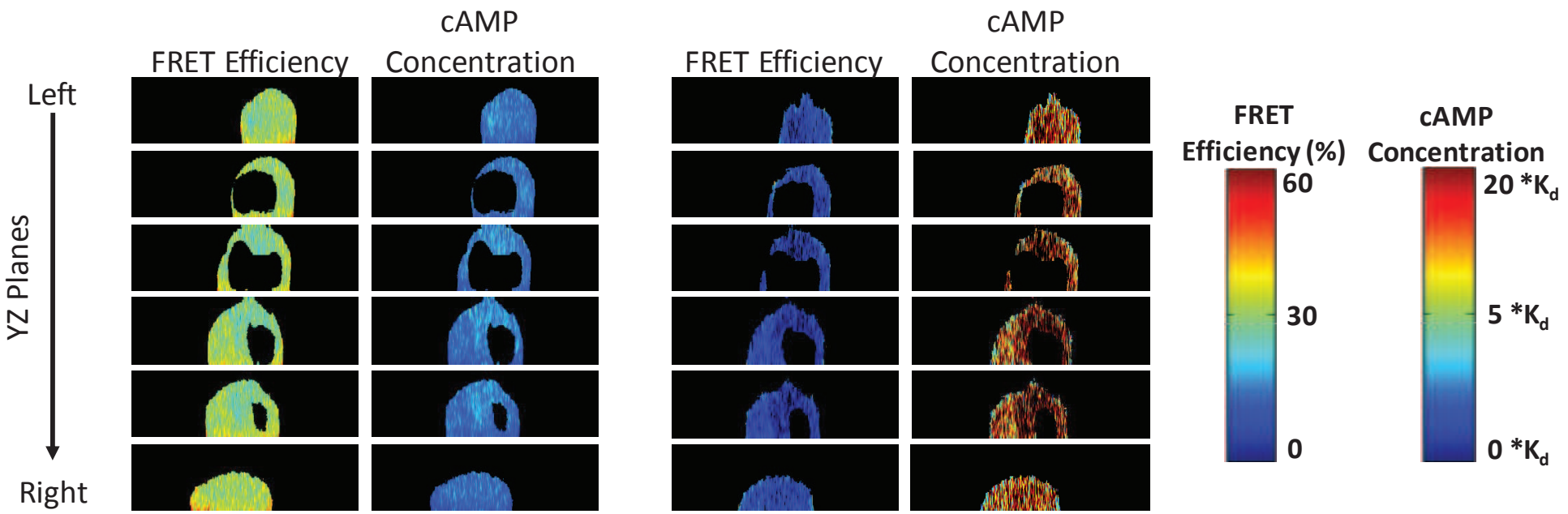

Figure 9

Click here to access/download;Figure;Figure 9.eps

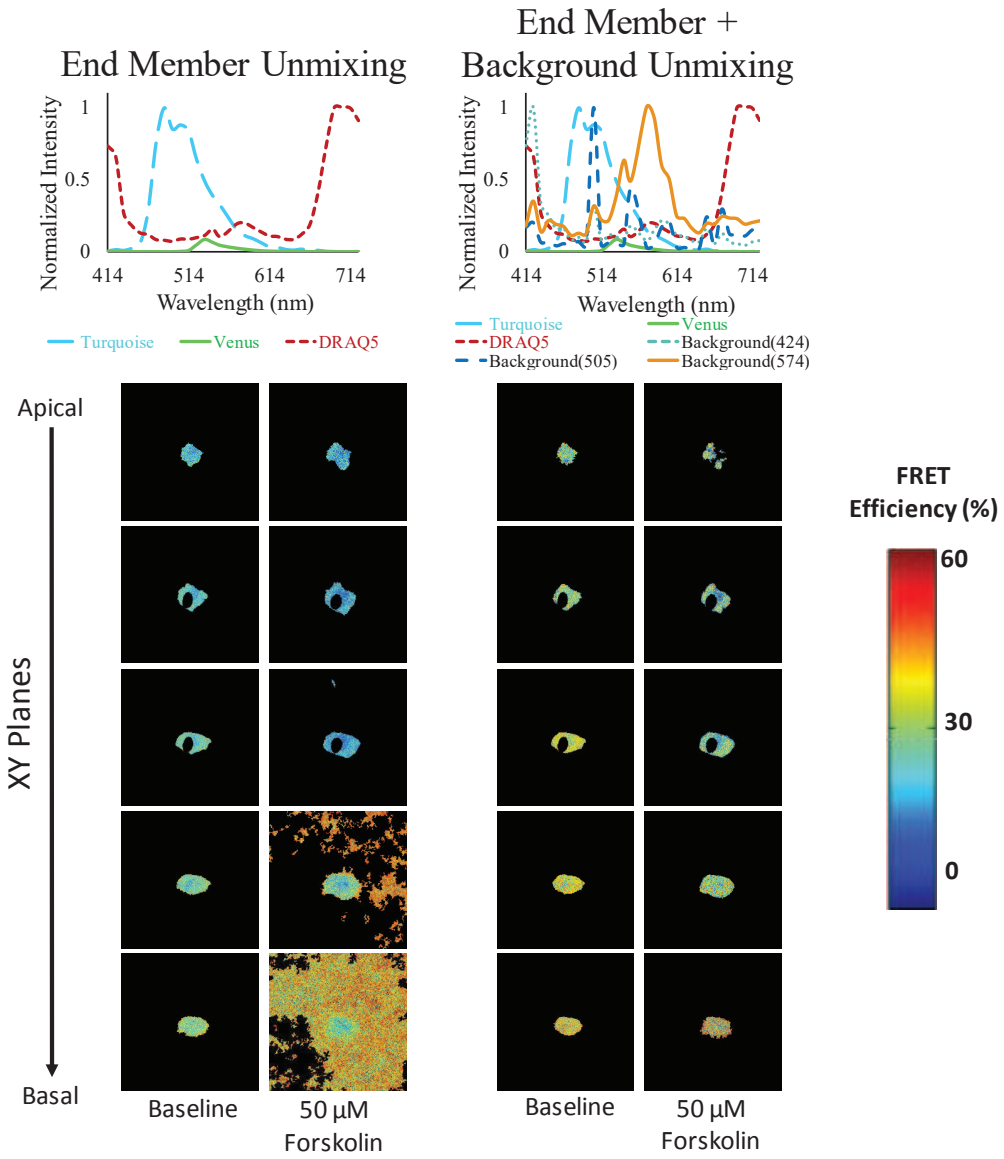

Figure 10

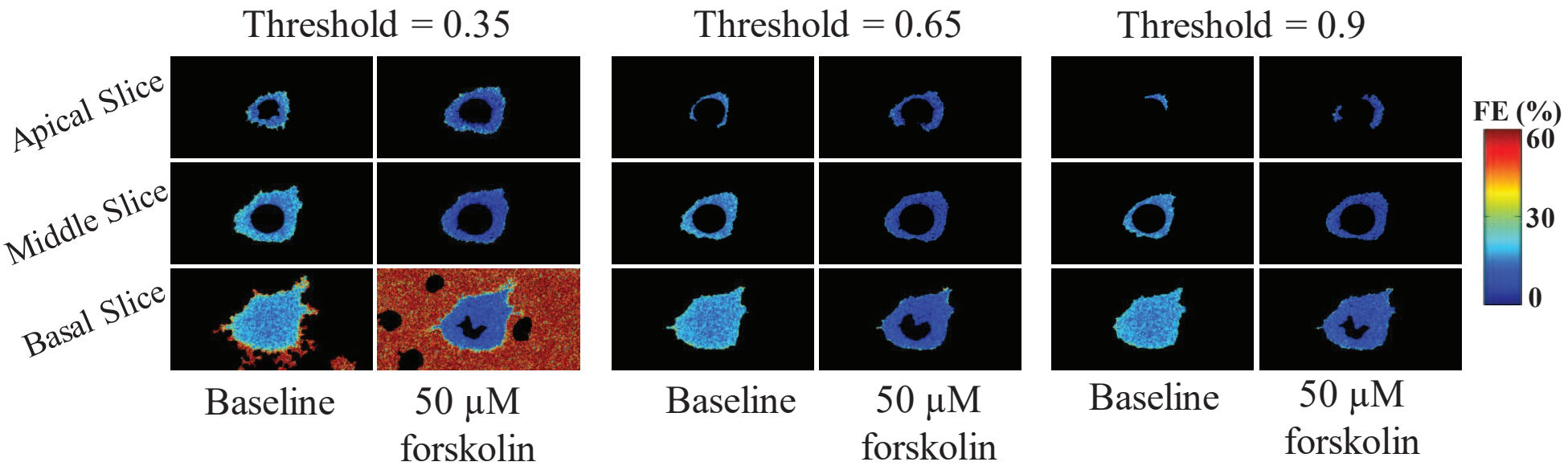

Figure 11

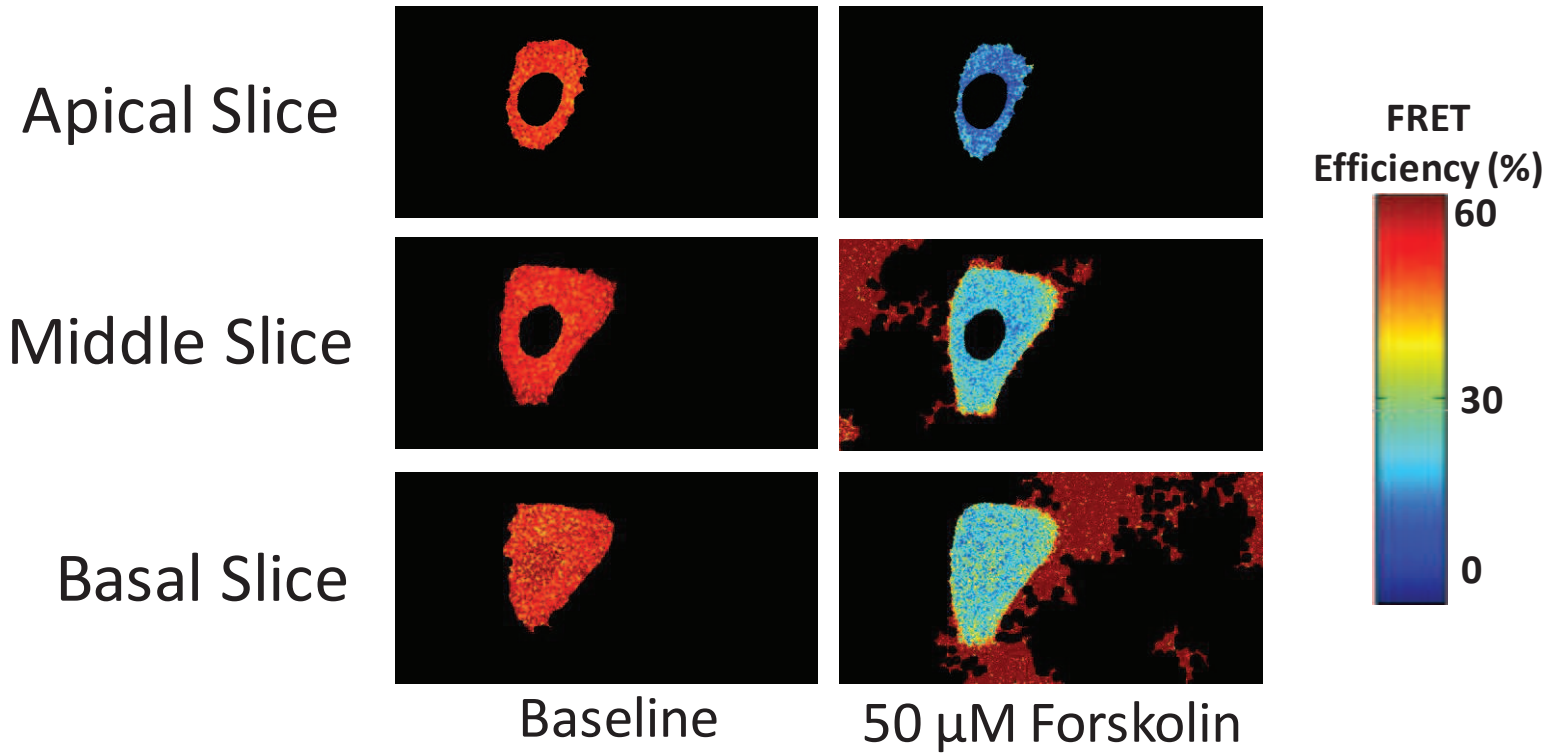

Supplemental Figure 1

Click here to access/download;Figure;Supplemental Figure 1.eps

A

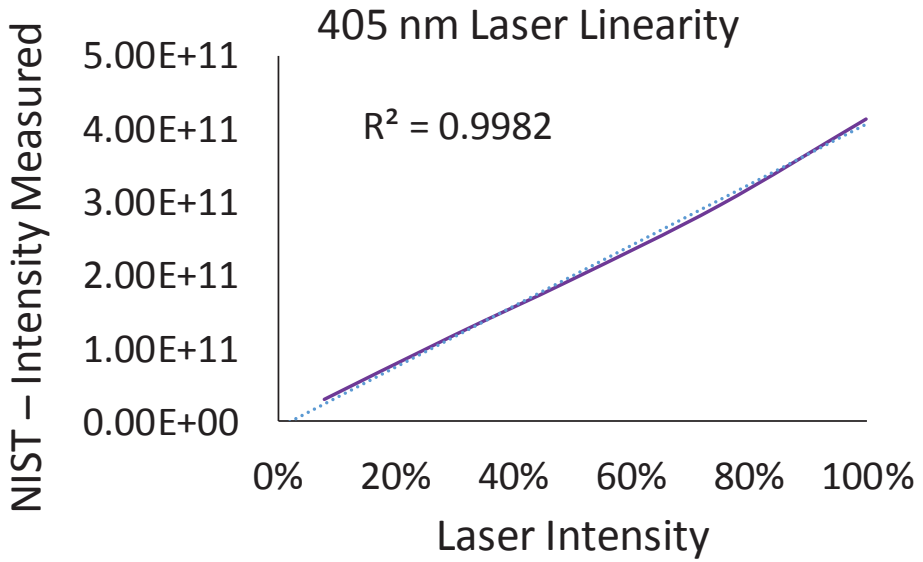

B

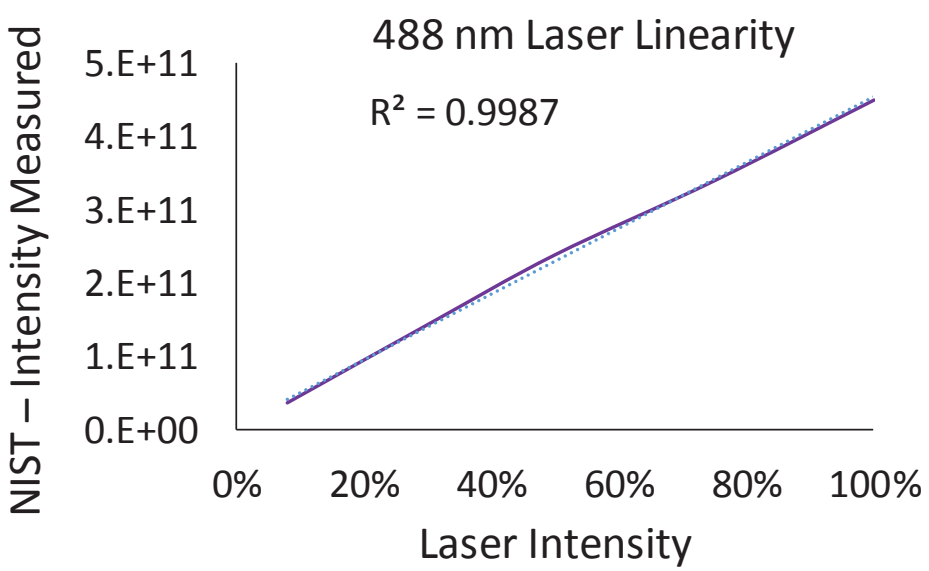

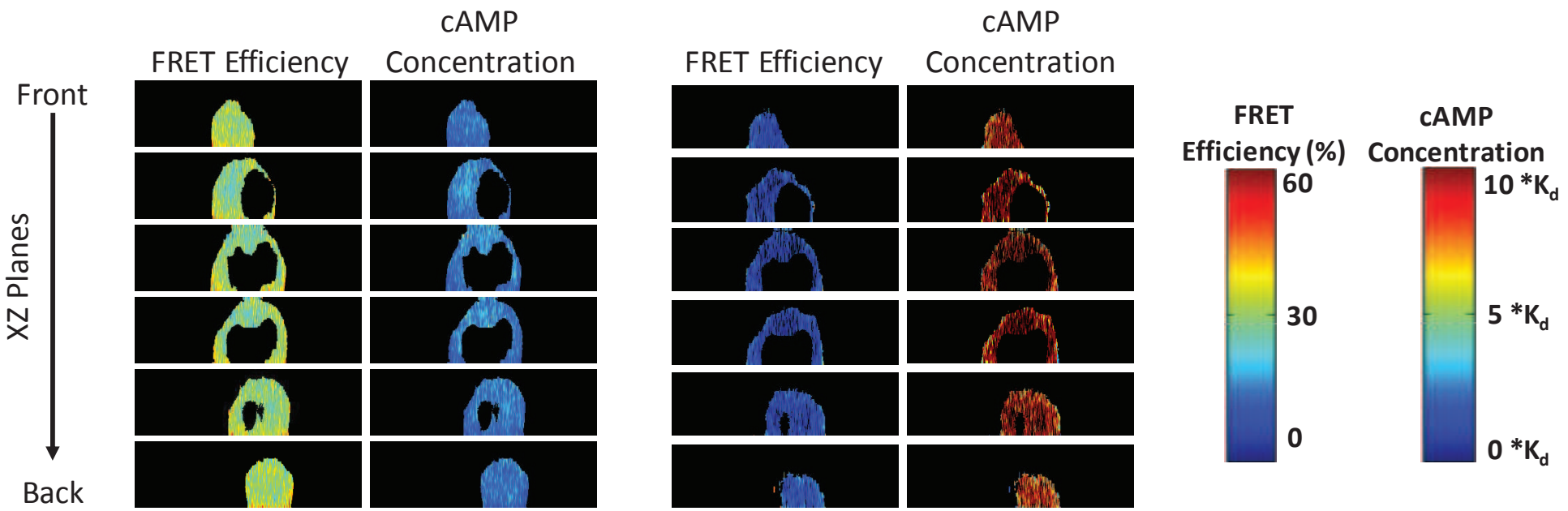

Table of Materials

Click here to access/download;Table of Materials;List of Materials.xlsx

Name of Material/ Equipment	Company	Catalog Number	Comments/Description
Attofluor Cell Chamber	Invitrogen	A7816	Attofluor contains steel cell chambers and a rubber O-ring. Cell chamber holds the coverslip and O-ring provides a lock in mechanism to hold the buffer in cell chamber with out leakage
Dimethyl Sulfoxide (DMSO)	Fisher Scientific	BP231-100	Solvent used to prepare stock solution forskolin.
DRAQ5 Fluoroscent Probe Solution	Thermo Scientific	62252	Nuclear label
Dulbecco Modified Eagle Medium (DMEM)	Gibco	11965-092	Contains nutrients and growth factors for the cells to grow and divide in the culture dishes.
Fetal Bovine Serum (FBS)	Sigma	F6178	Growth factor suppliment that is added to culture medium, DMEM
Forskolin	Sigma	F3917	Adenylv cyclase activator.
H188 Cyclic AMP FRET biosensor	Netherland Cancer Institute, Dr. K. Jalink	Gift	Plasmid encoding Turquoise (donor fluorophore), Venus (acceptor fluorophore), and binding domain obtained from Epac.
Image J	image.net	Free download	Another image processing platform used to extact spectral information and image processing.
Integrating Sphere	Ocean Optics	FOIS-1	Used to measure illumination intensity of the laser line at different laser intensities (?).
Laminin Mouse Protein, Natural	Invitrogen	23017-015	Coverslips are coated with laminin and this helps in cell attachment, growth and motility of the cell.
Lipofectamine 3000 Transfection Kit	Invitrogen	L3000-015	Transfection reagent used to transfect cells with H188 FRET biosensor
MATLAB	Mathworks	R2019a	Image processing operations (linear unmixing and FRET efficiency calculations) are performed by writing custom programs in MATLAB programming environment
Nikon A1R confocal microscope	Nikon Instruments	Nikon A1R	Spectral image acquisition is performed using confocal microscope.
Nikon Elements Software	Nikon Instruments	Software donale	used to exsort and handle nd2 image files (multidimensional image files) that are acuired usine Nikon A1R
NIST-Traceable Calibration Lamp	Ocean Optics	LS-1-CAL-INT	A lamp with a known spectrum for use as a standard
PBS pH 7.4 (1X)	Gibco	10010-023	coomonly used buffer suring cell culture
Pulmonary Microvascular Endothelial Cells (PMVECs)	In house - Cell culture core, Univerisity of South Alabama	Isolated from Rat pulmonary microvasculature	PMVECs form inner lining of a blood vessel.
Penicillin-Streptomycin (10,000 U/ml)	Gibco	15140-122	antibiotics are added to culture medium to prevent contamination of the cells.
Pre-Cleaned Gold Seal Micro Slides	Clay Adams	3010	Microscope slides used for cell fixation
ProLong Diamond Antifade Mounting Media	Invitrogen	P36961	If samples are fixed using antifade mountant, then the later protects fluoroscent dyes and chromophores from fading.
Spectrometer	Ocean Optics	QE65000	Used to measure spectral response of the light source (?)
Trypsin-EDTA (0.25%)	Gibco	25200-056	Digests the protein-protein bond between the cell and cell matrix and helps to dissociate and lift the cells during cell plating.
Tyrodes Buffer	Made in-house	Made in-house	Tyrodes buffer is used to make working solutions and to maintain cells in aqueous solution during image acquisition.
6 Well Cell Culture Plate	Corning	3506	Laminin coated coverslips are placed in 6-well culture dish (one coverlisps/well). Cells along with medium is added into each well.
25 mm Round Microscope Cover Slips	Fisher Scientific	12545102	Cells were grown on round glass coverslips
60X Oiective	Nikon Instruments	Plan Apo VC 60X/1.2 WI ∞/0.15-0.18 WD 0.27	water immersion and commonly used obiective for cells

RESPONSES TO THE COMMENTS FROM THE EDITOR:

Comment: Please take this opportunity to thoroughly proofread the manuscript to ensure that there are no spelling or grammatical errors.
Response: Thank-you for the careful review and critique of the manuscript. We have now proofread the manuscript to try to correct any spelling or grammatical errors.

Comment: Protocol Detail: Please note that your protocol will be used to generate the script for the video, and must contain everything that you would like shown in the video. Please ensure that all specific details (e.g. button clicks for software actions, numerical values for settings, etc) have been added to your protocol steps. There should be enough detail in each step to supplement the actions seen in the video so that viewers can easily replicate the protocol. Some examples.
1) Please include an ethics statement before your numbered protocol steps indicating that the protocol follows the animal care guidelines of your institution.
Response: An ethics statement has been added to the protocol.

2) 1.2: Mention culture media and growth conditions.
Response: Cell culture media and growth conditions have been added to the protocol. To further describe any details of cell growth conditions, a supplemental document was created for cell culture and transfection.

3) Your protocol exceeds the length limit of 10 pages. Please merge related steps so that each step has at most 3-4 related actions. Please consider splitting the protocol into 2 submissions.
Response: Our apologies for the oversight. We have reworked the manuscript to stay within the 10-page limit. Details of cell culture and transfection and construction of the spectral library have been added as supplemental sections with filenames called "Supplemental File_Cell Culture and Transfection" and Supplemental File_Spectral Library".

Comment: Protocol Highlight: After you have made all of the recommended changes to your protocol (listed above), please re-evaluate the length of your protocol section. Please highlight ~2.5 pages or less of text (which includes headings and spaces) in yellow, to identify which steps should be visualized to tell the most cohesive story of your protocol steps.
1) The highlighting must include all relevant details that are required to perform the step. For example, if step 2.5 is highlighted for filming and the details of how to perform the step are given in steps 2.5.1 and 2.5.2, then the sub-steps where the details are provided must be included in the highlighting. 2) The highlighted steps should form a cohesive narrative, that is, there must be a logical flow from one highlighted step to the next.
3) Please highlight complete sentences (not parts of sentences). Include sub-headings and spaces when calculating the final highlighted length.

4) Notes cannot be filmed and should be excluded from highlighting.
Response: Highlighting has been added to the relevant sections.

Comment: Results: Remove the numbering.

Response: The numbering in the results section has been removed.

Comment: Discussion: JoVE articles are focused on the methods and the protocol, thus the discussion should be similarly focused. Please ensure that the discussion covers the following in detail and in paragraph form (3-6 paragraphs): 1) modifications and troubleshooting, 2) limitations of the technique, 3) significance with respect to existing methods, 4) future applications and 5) critical steps within the protocol.
Response: The discussion section has been rewritten to focus on discussing details of the protocol/methodology, as suggested.

Comment: Commercial Language:JoVE is unable to publish manuscripts containing commercial sounding language, including trademark or registered trademark symbols (TM/R) and the mention of company brand names before an instrument or reagent. Examples of commercial sounding language in your manuscript are Lipofectamine 3000, Countess, MATLAB,
1) Please use MS Word's find function (Ctrl+F), to locate and replace all commercial sounding language in your manuscript with generic names that are not company-specific. All commercial products should be sufficiently referenced in the table of materials/reagents. You may use the generic term followed by "(see table of materials)" to draw the readers' attention to specific commercial names.
Response: We apologize for the oversight. All the commercial language/terms are now moved and restricted to "Table of Materials".

Comment: Table of Materials: Please sort in alphabetical order.
Response: The Table of Materials is now sorted in alphabetical order.

• If your figures and tables are original and not published previously or you have already obtained figure permissions, please ignore this comment. If you are re-using figures from a previous publication, you must obtain explicit permission to re-use the figure from the previous publisher (this can be in the form of a letter from an editor or a link to the editorial policies that allows you to re-publish the figure). Please upload the text of the re-print permission (may be copied and pasted from an email/website) as a Word document to the Editorial Manager site in the "Supplemental files (as requested by JoVE)" section. Please also cite the figure appropriately in the figure legend, i.e. "This figure has been modified from [citation]."

Responses to the Comments from Peer-Reviewers:

Reviewer #1:
In this article, the Authors report methodology for measurement and analysis of 3D cAMP distributions in living cells using hyperspectral FRET Imaging.
The methods are well described and the technic is of high interest and would be transposed to many cell types.
My comments are as follows:

Comment: Long abstract: please define SNR
Response: We now defined signal-to-noise ratio (SNR) in the long abstract.

Comment: Introduction, first paragraph: 21 references for 4 sentences. The Authors should select the most accurate ones.
Response: We agree with the reviewer and 14 accurate citations/references were selected out of previously cited 21 references.

Comment: L70-79 should not be part of the introduction, especially since the description of H188 (and all cAMP sensors) has already been reported.
Response: We removed the description of the cAMP sensor (lines 70-74) in the introduction. Since this is a methodology/protocol, we thought it still would be useful to retain a very brief description of what kind of FRET sensor was used in the study and how this sensor works in live cells to estimate cAMP levels.

Comment: L106-108: please provide references.
Response: References for lines 106 – 108 are now added

Comment: L150: « (explained in steps 1.3.131) » please correct
Response: This is now corrected. This part of the protocol section is now added to supplemental information with a file name called “Supplemental File_Cell Culture and Transfection” in response to comments made by the editor (above).

Comment: L156: Is the laminin-coated 6well-plate incubated for 1H at 37C? or RT?
Response: Laminin coated 6-well plates were incubated for at least one hour in the incubator at 37^0C. This is clarified in the protocol section (now moved to supplemental information with a file name called “Supplemental File_Cell Culture and Transfection”).

Comment: L167: what does 18.3 uL sensor DNA correspond to? what is the concentration of plasmid to add for 200 000 cells? If transfection tests are performed, the Authors should detail them.

Response: This is a good point. A plasmid concentration of 3 µg/ul was used to transfect pulmonary microvascular endothelial cells. This is now clarified, and the concentration of plasmid used has been added to the protocol section.
Yes, we have performed transfection tests with different concentrations of plasmid ranging from 2 to 5 µg/ul. Based on the transfection efficiency and expression levels of the probe in the cells, we selected 3 µg/ul as our optimal plasmid concentration to transfect the cells. These details have been added to the protocol section as well.

Comment: L177: which buffer are we considering here, please precise?
Response: We used Tyrodes buffer. A description of the buffer has been added to the protocol section.

Comment: L185: why not adding the DRAQ5 to the working buffer before, and add the mix to the cells?
Response: This is good point to note. For lightly adherent cells such as HEK293 cells, we have followed this procedure, as it is easy to lift the cells off of the coverslip. However, pulmonary microvascular endothelial cells (PMVECs) adhere well and we have found that DRAQ5 may be added directly to the attofluor. Adding directly to attoflour simply saves a step of mixing the buffer in a vial. We have added this note to the protocol as an alternate approach for labeling cells with DRAQ5.

Comment: L211: should the experimentator select a region with isolated cells? a brightfield image would help to visualize the region to select.
Response: We agree with the reviewer. Using brightfield mode helps to find an isolated cell easily. However, for a case where only a small fraction of cells express the FRET sensor, the selected cell that was identified using brightfield may not necessarily be a cell that is expressing FRET sensor. Hence, for cases where the transfection efficiency is (such as in PMVECs), we have found that using fluorescence mode is more helpful than using brightfield/white light mode, although the brightfield image can still be useful to confirm the boundary/extents of the cell.

Comment: L306: how is the reagent added ? perfusion system ? with pipet ? if so, how to ensure the proper dilution of FSK ? Is the diffusion of FSK into working buffer rapid and total (without shaking)?
Response: This is a good point. Our standard approach for PMVECs is to add forskolin in a sufficient quantity of buffer via pipet to ensure even mixing – this is clarified in the protocol section. In this case, a working concentration of forskolin is prepared in significantly large amount of tyrodes buffer (200 µL) and this reagent mixture is added to 800 µL of buffer present in the attofluor.

Comment: Figure 2 and legend: what is « baseline » ? vehicle ? please amend. The Authors should mention « vehicule/baseline » and « Fsk » on top of the images. Please indicate the image scale? Are we supposed to see a color (green) difference between the 2 images?
Response: Details for the figure and scale bar have been added to the figure.

This is a good point regarding color changes in the images. The 3D image projections shown represent raw spectral images (before unmixing) that have been false-colored using a wavelength-dependent color scheme generated in NIS Elements software. In summary, a false color is assigned to the image based on the fluorescence intensity at each wavelength (similar to a color projection through the wavelength space of the image). However, the changes in FRET are subtle enough that they result in very minimal changes to the projected color. This is one of the reasons why further analysis using linear unmixing and quantitation of the FRET efficiency is needed.

Comment: L331: which cell type?
Response: We used HEK293 cells to obtain the spectra of Turquoise and Venus for the spectral library. The cell type that was used to generate the spectral library has been added to the protocol.

Comment: L584: how accurate is the calculation of FRET signals to cAMP levels? -Would the technic be suitable for spontaneously beating cells such as neonatal cardiac myocytes or pacemaker cells?
Response: This is also a good discussion point. If the protocol is followed and FRET values calculated appropriately, conversion of FRET signals to cAMP levels are generally accurate. However, for spontaneously responding cells a faster image acquisition time would be desired, which would require a more sensitive detector as changes in FRET result in subtle changes in fluorophore intensity. Some newer model confocal microscope systems offer spectral detectors with InGaAs PMT arrays, which will offer improved sensitivity over the more traditional PMT array that is available on the Nikon A1R confocal microscope used in this study. Hence, studies on these systems may be able to be performed quicker, though likely still on the order of ~10-15 seconds per 3D spectral image stack.

Comment: The Authors did not mention any bleaching and Bleed-through corrections? please discuss.
Response: This is an excellent suggestion to include discussion about bleaching and bleed-through corrections. We and others have shown that spectral imaging followed by linear spectral unmixing effectively account for bleed-through concerns that were typical of more traditional 2- or 3-color/channel detectors. We have previously worked to characterize the photobleaching properties of the FRET sensor as expressed in PMVECs. Photobleaching studies displayed very little/no photobleaching (<1%) of Turquoise and Venus fluorophores within 10 minutes (~3 minutes baseline acquisition+10 minutes wait time with lasers off+~3 minutes after treatment image acquisition). Hence, we did not include a discussion of photobleaching in the original manuscript. However, to address these concerns we have now added further points to the discussion section.

Comment: The Authors should provide a sequence of FRET data obtained with increasing concentrations of Fsk or isoproterenol, in order to have an idea of the dynamics of the probe in these technical conditions. How sensitive can be the response?

Response: This is also a good point. Dose response studies have been previously performed and are reported in Leavesley et.al., Cytometry A,83A: 898 - 912, 2013. Hence, we have not included them in the manuscript.

Reviewer #2:

Manuscript Summary:

FRET-based measurements in living cells have revolutionized cell biology and cell signalling research. However, FRET-based sensors for cAMP, despite significant efforts from different laboratories, still present a number of limitations, including low signal-to-noise ratio (SNR) and low spatial signal detection. In this manuscript the authors present a comprehensive protocol for the implementation of FRET with hyperspectral imaging approaches. The most obvious limitation of this approach is the loss of fast dynamic cAMP changes since a temporal scale in the order of minute is more applicable than seconds. The protocol is comprehensively written and can be easily followed, moreover it is enriched with helpful tips and considerations. I have only some minor comments:

Major Concerns:

None

Minor Concerns:

Comment: The authors define cAMP as a "second messenger signal", it may be semantics from my part, but second messengers act as signals, therefore it would be more fitting define cAMP as "second messenger".

Response: We agree with the reviewer. cAMP is now defined as a “second messenger” in the manuscript.

Comment: The authors, in several parts of the manuscript refer to FRET measures of cAMP as "cAMP concentration", this is not the case. The authors did no calibration of the sensors with known doses of cAMP. Moreover, FRET sensors measure only free cAMP therefore can provide only an approximation of the cAMP cellular levels (which include the messenger bound to its buffers).

Response: We agree with the reviewer and apologize for any confusion. For this cAMP sensor, the Hill equation was used to map the fraction of receptor occupied by ligand (FRET efficiency in this case) to the concentration of ligand (cAMP in this case) and the dissociation constant (Kd). However, because the dissociation constant of the FRET reporters in PMVECs and in different compartments of the cell is not exactly known, we have described our cAMP “concentrations” as normalized/relative to the value of Kd. To avoid any further confusion, the term “cAMP concentration” has been changed to “cAMP level” throughout the manuscript.

Comment: In line 243 point 3.12.1 the authors advice for the laser intensities to be adjusted based on the age of the instrument and condition of the lasers. It would be advisable for the authors to add a note on the importance to obtain

comparable expression levels of the sensor(s) between different experimental days.
Response: The advice regarding laser intensities was included to make potential users aware that this is an important factor that may vary from instrument to instrument, and even on the same instrument over long periods of time (months-years). For experiments described in this methodology, all intensity values were kept constant across all trials (i.e., across all experiments run on different days). We agree with the reviewer that the expression levels of the FRET sensor may vary from day to day, or even from cell to cell (we have in fact observed this) – but in constructing a repeatable methodology, we feel that it is important for users to maintain similar equipment settings and to then select cells with similar expression levels (as opposed to altering equipment settings to compensate for expression level). Hence, we advise users to use similar settings for image acquisition across all experiments.

Comment: In line 356 (4.12) the specific quantity in µl is missing
Response: The quantity has been added.

Comment: In lane 45 there is a "to" that has to be eliminated
Response: "to" has been removed.

Comment: 50µM FSK is too much, 10µM to 20µM FSK is saturating for virtually every cell line. In fact, it is surprising that the authors are able to dissect cAMP gradients in the apical to basal axis after 10-minute treatment with FSK 50µM. It would have been exceptionally informative to repeat the same experiment treating the cells with FSK 50µM and a PDE inhibitor to block the enzymes (PDEs) most likely responsible for the gradient formation.
Response: This is a good point, and is something we have considered. In fact, we have performed experiments similar to this using PGE_1 and PDE inhibitors. We treated cells with saturating concentration of either PGE_1 (25 µM) or Rolipram (10 µM) alone and observed existence of spatial cAMP gradients. When cells were treated with 25 µM PGE_1 + 10 µM Rolipram, gradients were completely abolished (see figure below).

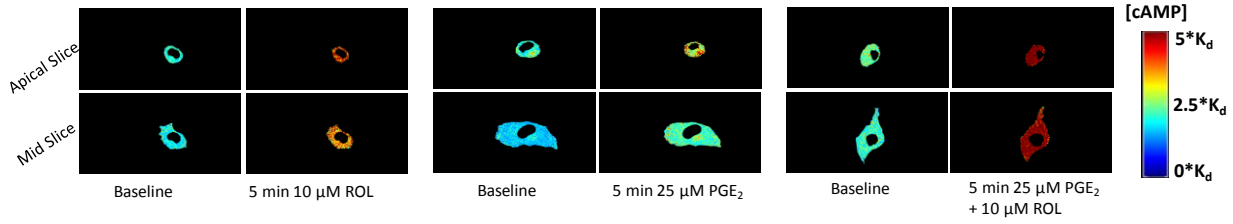

Reviewer #3:
Manuscript Summary:
The manuscript is very detailed and presents and interesting application of multispectral

FRET analysis, that allows to increase the signal/noise ratio that is always a problem in FRET analysis done on single cell. The proposed method required a suitable confocal microscope and a sophisticated computer facilities, and therefore is useful only for specialized laboratories

Major Concerns:
Comment: The presented examples are not very clear, at least for the present referee...I was not able to see any difference in cAMP (and FRET) in the Z slices presented in fig. 7 and 8 . Where is the claimed spatial distribution of cAMP? Are more informative examples of 3D distribution available??
Response: Visualization of cAMP gradients is a valid comment. When applying a colorbar to cAMP level images for visualization, the upper limit of the grey scale cAMP level was set to 10*Kd. That means, any pixel with a grey scale value ≥ 10*Kd is assigned a red color. In Figure 7, the cAMP concentration increased up to 20*Kd after treatment with forskolin. This resulted in a constricted colorbar (oversaturated in the color lookup space) that reduced the ability to visualize the spatial gradient clearly. We have now adjusted the color bar where cAMP spatial gradients can be clearly seen in Figures 7 and 8. As a suggestion from another reviewer, we have also added a line profile plot to Figure 7, to better demonstrate the quantitative nature of the spatial variations in cAMP signals along the length of the line.

Minor Concerns:
Comment: In the methods additional information should be given on the composition of growth media (pag3 line 118 and pag 4 line 124) and of working buffer (page 6 line 182 and 191) really 800 ml of buffer were used?
Response: Additional information on the composition of growth medium and Tyrodes buffer has been added to the section on cell culture which has now been moved to supplemental information to allow for a higher level of detail. It was a typo where 800 800 µl was mistakenly typed as 800 ml (now corrected). The more detailed protocol section is now contained in a file named “Supplemental File_Cell Culture and Transfection".

Reviewer #4:
Manuscript Summary:
This is important and interesting manuscript describing a hyperspectral FRET imaging methodology to visualize and quantitate FRET imaging and analysis. Authors address important issues such how to calculate FRET efficiencies with spectral specificity and to spectrally separate FRET signals from confounding autofluorescence and/or signals from additional fluorescent labels. Some details on trypsinization and cell culture may be to detailed considering that they are such standards methods. Also relying on Nikon software and Matlab may restrict the number of users, so it would be suggested that alternatives are pointed out to users that may not have access to these softwares.

Minor Concerns:

Comment: 2.2) Mount a coverslip containing transfected cells into a cell chamber (attofluor) and secure the top with mounting gasket to prevent leaking.

- what is attofluor and why and how it is included here?

Response: Attofluor (ThermoFisher) is a coverslip holder designed to hold a 25 mm round coverslip as well as buffer for live cell imaging (see figure below). The attofluor is used by placing the coverslip containing cells in the lower chamber and firmly fastening the upper chamber. Buffer may then be added in the upper chamber where a rubber ring forms a seal between the upper chamber and coverslip to prevent leakage.

Attofluor cell chamber.

Source of the figure: https://www.thermofisher.com/order/catalog/product/A7816#/A7816

Comment: 3.11.2) Under the A1 settings menu, check the boxes corresponding to 405 nm (for Turquoise, donor excitation) and 561 nm (for DRAQ5, nuclear label excitation) laser lines for sample excitation.

- Prevent cross-bleedthrough between 561 nm (for DRAQ5, nuclear label excitation) laser line and Venus from FRET sensor? Address this question, please.

Response: In the interest of a thorough discussion this point should be clarified – thank-you. The 405 nm laser was used for donor (Turquoise) excitation and the 561 nm laser was used for DRAQ5 excitation. However, it is conceivable that either the 405 nm laser or even the 561 nm laser could potentially directly excite Venus, though at very low efficiencies. In prior control studies, we have evaluated the excitation spectrum of the previous generation CFP-EPAC-YFP cAMP FRET sensor using spectrofluorimetry (Leavesley, et al., Cytometry A, 83A: 898-912, 2013) and found that YFP (similar to Venus) excites at only 0.5% efficiency at wavelengths of 415 nm or below (relative to 100% at the excitation peak). By contrast, CFP (similar to Turquoise) excites at 63% efficiency at 415 nm. Hence, signal generated by CFP excitation should be ~120X that of the signal generated by direct YFP excitation and this effect was deemed negligible. In addition, in separate photobleaching studies we do not see any emission of the Venus fluorophore at 561 nm laser excitation.

Comment: 3.12.3) Select a pinhole radius of 2.4 airy disk units.

- Why? Please explain why the choice of 2.4 AU

Response: We thank the reviewer for the suggestion here and in the next few comments to explain/elaborate on the specific numbers for each imaging parameter. The pinhole size of 2.4 AU was selected as a compromise that ensured acquiring a

spectral image with required signal-to-noise ratio (SNR) while preserving some measure of confocality (optical sectioning). As the reviewer is aware, increasing the pinhole size will increase the signal available for measurement, and hence increase the SNR making FRET claculations more sensitive, but will decrease the confocality. Confocal microscope users often use pinhole size ~1.5 or lower. However, FRET signals are inherently weak and offer low SNR. Hence, using a marginally wider pinhole diameter may help to improve SNR. Details on why this pinhole size was selected have now been added as a note in the protocol.

Comment: 3.12.4) Set the scan speed to 0.25 (0.25 spectral frames per second).
- Why? Please explain why the choice
Response: With scan speed of 0.25 it took ~3 minutes to acquire a spectral z-stack. We found this to be a reasonable compromise between imaging speed and SNR with minimal photobleaching. Increasing scan speed would reduce the time required for acquiring a spectral z-stack, but at the expense of reduced SNR. Likewise, increasing the laser excitation power would increase the SNR, but at the expense of increased photobleaching. A note has been added to the protocol to clarify these details.

Comment: Note: A 1 µm step size was selected as a compromise between imaging speed, z-axis sampling, and photobleaching. For very stable samples where speed is not critical, a smaller z-axis step may be used to increase z-axis resolution.
- Should the authors consider to image the sample under Nyquist resolution for x,y and z? In particular for z-steps using Nyquist resolution is advised.
Response: This is also a very good point and related to the 2 above points. We have selected a z-step value so as to compromise between acquiring a z-stack fast enough to ensure minimal photobleaching or motion artifacts and achieving a high z-axis resolution. The confocal pinhole diameter of 2.4 AU resulted in an optical section thickness of 1.73 um. We used z-step interval of 1 um (scanning every 1 um in z-direction), which is not quite Nyquist criteria, due to this need to compromise between imaging time, photobleaching, and resolution.

Comment: The Turquoise and Venus spectra for the library were acquired using cells expressing the H188 FRET reporter.
- Authors should suggest controls for FRET validation as available in Addgene
- Also how are individual turquoise and venus spectra acquired?
Response: The reviewer is correct – the spectra for Turquoise and Venus were acquired from the H188 FRET reporter. This is intentional, and arose out of discussions with several colleagues and from review of our previous paper (Annamdevula, et al., 2018). In summary, to be able to calculate the actual FRET efficiency (as opposed to an arbitrary FRET index), the individual spectra of Turquoise and Venus should be measured under equimolar conditions. Because it is difficult to know the absolute concentration of individual fluorescent proteins within a cell, we decided to use the H188 probe in order to maintain a 1:1 stoichiometry between donor and acceptor fluorescent

proteins. To then measure the individual spectra of Venus and Turquoise, we utilized a photobleaching approach. The donor+FRET spectrum was first measured by excitation at 405 nm and used as a reference. The direct excitation and emission of the acceptor was then measured by excitation at 488 nm. The acceptor was then photobleached using the 514 nm laser. Finally, the donor spectrum was measured by excitation at 405 nm and compared to the initial donor+FRET spectrum to ensure that the donor peak had increased and the acceptor peak had vanished. In this way, donor and acceptor spectra could be measured while ensuring equimolar concentration. This approach is described in detail in a revised protocol section that has been moved to supplemental information due to its length (see the file named "Supplemental File_Spectral Library"). Note that individual Turquoise and Venus constructs are available, and we have purchased them ourselves, but it will be very difficult to guarantee equimolar concentration when using them and hence, results will likely not be able to be calculated in terms of an absolute FRET efficiency. For reference, the spectra of Turquoise and Venus as measured from individual constructs that we purchased from Addgene are shown below. Note that the single construct spectra for Turquoise and Venus (dashed lines in blue and green) were both normalized to a peak intensity of unity because their fluorescence emission was measured in arbitrary units and the concentrations of fluorescent proteins within the cell were unknown. By contrast, the spectra measured from the H188 probe is presented where Turquoise is normalized to a peak intensity of unity, but the peak intensity of Venus is lower, as it has been measured at equimolar concentration with Turquoise.

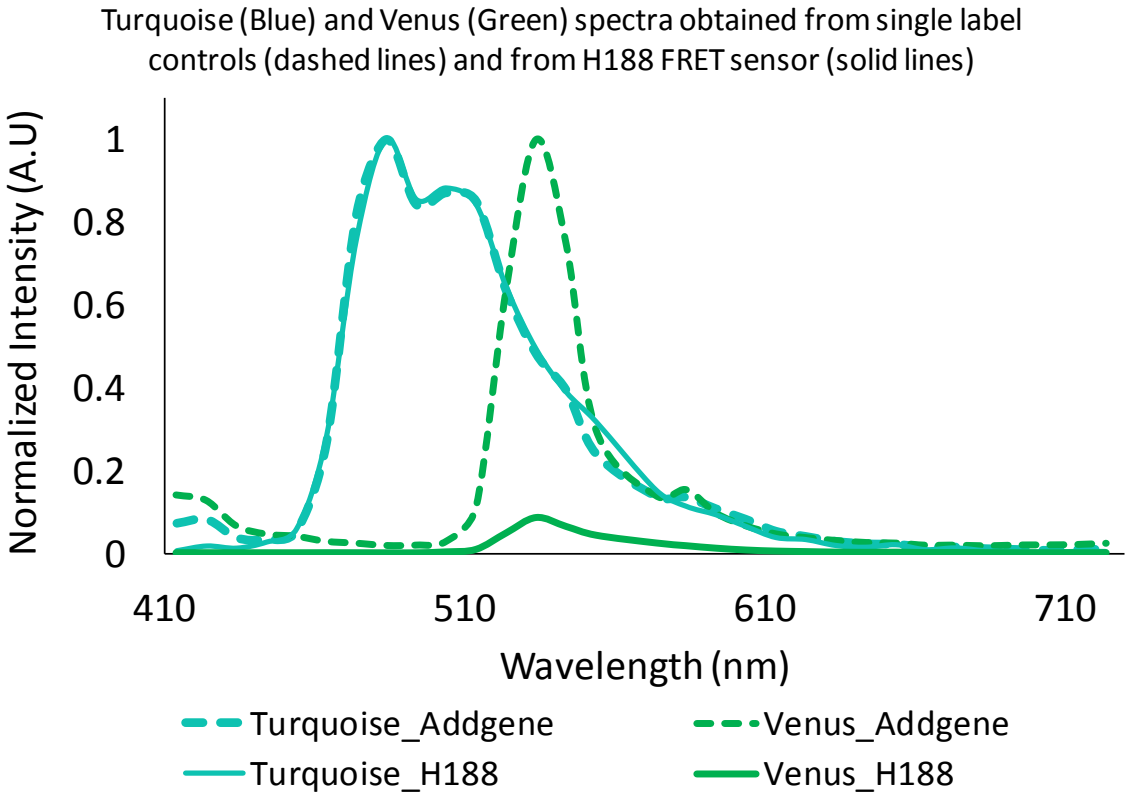

Comment: **Note: Complete photobleaching of acceptor takes at least an hour. In our studies, acceptor fluorophore is completely photobleached (no acceptor signal seen when excited using 488 or 405 nm lasers) in 1.5 hour.**
- This is not acceptable. Not sure why this is happening, but 1 hour of straight illumination for complete bleaching is not acceptable since that will lead to irreparable cell damage. Authors need to propose alternatives or inquire why photobleaching is taking so much time.
- Acceptor photobleaching is also not well introduced and explained. Why is being performed and for what goal and to address what question?
Response: This does appear to be a long period required to photobleach the acceptor, and we have questioned it ourselves. However, in our repeats of 3 experiments, it always took at least 1 hour to completely photobleach Venus. This may be due to the fact that our confocal microscope is relatively old (now at ~10 years) and the 514 nm line is quite dim. It may take a shorter amount of time to photobleach Venus on other systems. For an explanation of the rationale behind Venus photobleaching when constructing the spectral library, please see the response to the question above. We have added a note to the protocol to address these concerns and this section on forming the spectral library may now be found in the file named "Supplemental File_Spectral Library".

Comment: Authors state imaging parameter choice without explaining how to select the values. They caution readers that values may need to be adjusted but do not explain the main factor that may affect this choice. This prevents readers from understanding how to apply this methodology to their specific samples.
Response: We thank reviewer for this concern. It is very important to add in details on how imaging parameters should be adjusted instead of just blindly using a predefined value. As discussed in above comments, we have now added details and notes to the protocol on how these parameters effect image acquisition depending on the sample and fluorophores used.

Comment: Specific requirements for use of Matlab may reduce usage from audience since not all users have access to Matlab license
Response: It is true that there may be some users without access to MATLAB. However, the analysis described in the protocol may also be performed using alternative platforms such as imageJ, Python, cell profiler, etc., that are freely available. We have amended the protocol to state that image analysis can be performed using other image analysis platforms, and to alert readers to the availability of other image platforms that can perform this kind of image analysis.

Comment: **Figure 2 does not provide any extra information that it is not included in Fig 5A and thus should be removed**
Response: We agree with the reviewer. However, we thought it would be nice for the reader to visually see how a z-stack projection would look before and after treatments.

As a result of other reviewer comments, we have now added more information to the figure panels, and they are now quite different.

Comment: Figure 3 legend is not clear. Please explain the ROIs 1-4 and correlate them with the spectra graphs
Response: The figure caption/legend has now been amended to better describe the ROIs and to correlate them with the spectra graphs.

Comment: Need to stress that thresholding is just used to select cells not to be applied to the collected data for FRET analysis.
Response: We have clarified this portion of the protocol and the corresponding results section to state that thresholding was performed only for creating a cell mask.

Comment: Quantitative approaches should be provided to analyze the data included in Figure 7-8. FRET is a quantitative imaging assay and thus there should be way to collect quantitative data from these images
Response: We agree. Since this was a protocol-focused manuscript, we did not concentrate on showing a large amount of quantitative data. However, it is valuable to remind readers as to the quantitative nature of the image data. Figure 7 has now been revised to demonstrate one approach to visualize and work with quantitative FRET/cAMP data (visualization of data using a line scan).

Reviewer #5:
Traditionally, 3D FRET imaging has not been widely utilized due to difficulties in resolving the FRET signal from low SNR images of individual z-slices and other minor but important possible sources of signal contamination that has to be taken into account. The manuscript by Annamdevula et al describes methods of quantitating 3-D profile of cAMP concentration within a cell. The method utilizes a spectral detector that many of more recent confocal microscope systems are equipped with and thus should be practical for many that already have some experience in 2D FRET imaging and want to expand their analysis to spatially resolve subcellular distribution of the signals of interest.

The method is very well described. I only have a minor question and two minor points.

Comment: Lines 361-365, 4.15, 4.16:
Are XY images of a blank coverslip and a coverslip with no-labelled cells acquired using both 405 and 561nm lasers as in 4.14)? Whether the laser should be switched or not was not clarified.

Response: Yes, similar image acquisition settings were applied to acquire sample blank images. Both the 405 nm and 561 nm lasers are turned on simultaneously for the acquisition of these control images. A sentence clarifying this is added to the protocol, where the corresponding section on forming a spectral library has now been moved to a file labeled “Supplemental File_Spectral Library”.

Comment: Lines 526, 5.2.6): The rectangular selection tool is somewhat difficult to adjust the size at the pixel level. I would recommend describing "Specify" command (Edit -> Selection> Specify) to set a region so that a ROI of the same dimension can be easily be defined and used over many separate images.
Response: This is a good point. We have added a comment saying that the Specify Selection tool may also be used to accurately define the size of a rectangular ROI.

Comment: Lines 450、463: photos -> photons
Response: This has been corrected.

Supplemental Information - Cell Culture and Transfection:

Cells and cell type may vary from study to study and hence cell-specific cell culture procedures should be followed to seed and grow cells. Pulmonary microvascular endothelial cells (PMVECs) were used to study the cAMP spatial distributions shown in the manuscript titled "Measurement of Three-Dimensional cAMP Distributions in Living Cells Using 4-Dimensional (x, y, z, and λ) Hyperspectral FRET Imaging and Analysis". This supplemental file provides detailed information on the cell seeding, cell culturing, and cell transfection protocols used.

Rat PMVECs were isolated as described previously[1] and maintained in medium (refer to "List of Materials" for details on the medium used) supplemented with 10% (vol/vol) fetal bovine serum (Gemini), 100 U/ml penicillin, and 100 µg/ml streptomycin, pH 7.0 until cells attained 100 % confluency. Cells were seeded on 25 mm round glass coverslips for imaging as described below.

1) Cell Splitting:

1.1) Aspirate media from the dish.

1.2) Rinse cells with PBS buffer.

1.3) Add 1 ml trypsin containing 0.25 % EDTA and incubate for 5 min at 37 °C.

1.4) Add known volume of media (this volume will be used to calculate concentration of cells in later steps) containing fetal bovine serum to arrest the action of trypsin.

1.5) Resuspend cells into a conical.

1.6) Count cells using a cell counter as follows.

Note that there are several alternative ways to perform cell counting for cell culture. Here, we describe use of an automated cell counter.

1.6.1) Gently mix resuspended cells by tapping the bottom of the conical.

1.6.2) Take 10 µl of resuspended cell media into a vial and add 10 µl of trypan blue and mix gently using the same pipette.

1.6.3) Take 10 µl of this mixture (cell media and trypan blue) and pipet into a disposable cell counting chamber slide.

1.6.4) Insert the slide into the cell counter.

1.6.5) Wait for 10 seconds and record the total number of viable cells. It is recommended to take picture of the cell counter screen for laboratory records.

1.6.6) Centrifuge resuspended cells (remaining cell suspension after step 1.6.2) at 135 × g for 10 minutes. Make sure to note the volume of the cell suspension by reading the volume present in the conical. This is used to calculate the total number of cells present in the cell suspension.

1.6.7) Carefully remove the supernatant, so as to not disturb the cell pellet.

1.6.8) Calculate the total number of cells in the cell pellet using the recorded values. For example, if the volume of cell suspension that is centrifuged is 5 ml and total viable cell count is 1 million cells/ml (from cell counter in step 1..6.6), then the total number of cells in the cell pellet after centrifugation will be 5 million cells.

1.6.9) Resuspend the cell pellet in 1 ml of media. This establishes the working concentration of cells – as an example, 5 million cells/mL based on the above example calculation.

1.7) Plate 200,000 - 250,000 cells/well on prepared laminin coated coverslips (explained below).

1.8) Laminin Coated Coverslips:

1.81) Place one 25 mm round glass coverslip in each well of a six-well plate.

1.8.2) Dilute laminin in PBS buffer to make a final concentration of laminin of 5 µg/ml.

1.8.3) Add 1 ml of 5 µg/ml laminin solution to each well of the six-well plate to coat the coverslips.

1.8.4) Incubate the six-well dish containing laminin coated coverslips for at least 1 hour at 37^0C. Note that the laminin coated coverslips can be used even after longer incubation times.

1.8.5) Pipette off the laminin solution after $\geq$ 1-hour incubation and wash 3 times with buffer (PBS) before using for cell seeding.

1.8.6) Incubate for 24 hours at 37 ^{0}C or until the cells attain 70-80% confluency.

2) Cell Transfection: Transfect the cells with the FRET sensor using transfection solution, as described below.

Note: The transfection reagent used in these studies comes as solutions: Solution A and Solution B. Please refer to “Table of Materials” to see details about the transfection reagent used.

2.1) Take two test tubes (mark A and B) and add 750 µl of media to each test tube.

2.2) Add 20.5 µl solution A to test tube A and gently mix by tapping the test tube.

2.3) Add 18.3 µl (3 µg/µL) of FRET based biosensor plasmid (DNA) and 30 µl of solution B to test tube B and mix by tapping the tube.

Note: We have performed transfection tests with different concentrations of plasmid ranging from 2 to 5 μg/μl. Based on the transfection efficiency and expression levels of the probe in the cells, we selected 3 μg/μl as our optimal plasmid concentration to transfect the cells. The concentration of plasmid DNA used is to attain optimum transfection in PMVECs – it may be necessary to modify this concentration for another cell line or cell type.

2.4) Mix contents in test tube A and B and incubate for 5 minutes at room temperature.

2.5) Add 250 μl of the mixture to each well of a six well dish containing cells grown on laminin-coated coverslips. Note: The volumes of media, DNA, and transfection reagent described here are sufficient to transfect 6 coverslips.

2.6) Incubate cells at 37 °C for 48 hours.

References:

1. Thompson, W. J., Ashikaga, T., Kelly, J. J., Liu, L., Zhu, B., Vemavarapu, L. & Strada, S. J. Regulation of cyclic AMP in rat pulmonary microvascular endothelial cells by rolipram-sensitive cyclic AMP phosphodiesterase (PDE4). *Biochemical Pharmacology* 63**,** 797–807 (2002).

Supplemental Information: Spectral Library Construction:

A spectral library consists of pure spectra of each fluorescent label present in the sample and spectra of non-specific background signatures if any (for example, in these studies, the spectral library consists of Turquoise, Venus, and DRAQ5, as well as background spectral signatures from the cell matrix or autofluorescence, coverslip fluorescence, and reflection from the coverslip). The protocol described in this supplemental file corresponds to steps involved in construction of spectral library to perform spectral unmixing on the image data acquired in the actual manuscript titled "Measurement of Three Dimensional cAMP Distributions in Living Cells Using 4-Dimensional (x, y, z, and λ) Hyperspectral FRET Imaging and Analysis". The Turquoise and Venus spectra for the library were acquired using HEK293 cells expressing the H188 FRET reporter. For FRET efficiency measurements, the concentration of donor and acceptor fluorophores in the sample should be equal. If single label Turquoise and Venus constructs were expressed in cells (even using equal concentrations), the expression of these fluorophores would likely not be 1:1 stoichiometry. Hence, to meet this criterion we used cells expressing the H188 FRET sensor. FRET sensors express as a single molecule in the cell and hence the concentration of Turquoise and Venus in the cells will be the same (i.e., fixed 1:1 stoichiometry). The steps involved in constructing the spectral library are described below:

1) Cell or Sample Preparation:

1.1) Seed Human Embryonic Kidney 293 cells (HEK293) on 20 mm round glass coverslips in a 6-well dish.

1.2) Maintain cells in minimal essential medium (MEM, containing 10% v/v fetal bovine serum) for 24 hours or at least cells attain 60-70% confluency at 37^0C in an incubator.

1.3) Transfect three out of six wells from step 1.1 with 3 µg/µl FRET biosensor (this yields 3 coverslips containing expressing cells and 3 coverslips containing control or non-expressing cells).

1.4) Incubate cells for 48 hours at 37^0C in an incubator.

Note: The detailed step-by-step procedure for cell seeding and cell transfection (for steps 1.1) through 1.4)) are available in the supporting/supplemental file named "Supplemental File_Cell Culture and Transfection".

1.5) Fix HEK293 cells expressing FRET biosensor to obtain Turquoise and Venus controls:

1.5.1) Clean the microscope slide using alcohol swab to make sure that the slide is clean and that there are no dust particles.

1.5.2) Add a drop of mounting medium on the microscope slide.

1.5.3) Gently remove the coverslip containing expressing cells using lab tweezers and place the coverslip on the microscope slide containing the mounting medium.

Note: Make sure that the face of the coverslip containing cells should be facing the microscope slide/mounting medium. Please refer to “List of Materials” for mounting medium used in these studies.

1.5.4) Allow the fixed cells to cure for 24 hours in a dark place.

1.5.5) Apply clear nail polish along the edge of the coverslip such that the coverslip is adhered to the microscope slide.

1.5.6) Allow the nail polish to dry for few minutes.

1.6) Prepare DRAQ5 single label control cell sample using non-expressing HEK293 cells.

1.6.1) Place a coverslip containing non-expressing HEK293 cells in a cell chamber.

1.6.2) Add 4 µl of 5mM nuclear label to 800 µl of buffer and vortex for few seconds for uniform mixing of the dye in the buffer.

1.6.3) Add the nuclear label-buffer mix to the cell chamber and incubate for 10 minutes at room temperature.

1.7) Place coverslip containing non-expressing cells in a cell chamber and cover with 800 µl of buffer. This will be used as autofluorescence single label control.

1.8) Place a plain and clean 20mm round glass coverslip in a cell chamber. This will be used as a control to obtain spectra for coverslip fluorescence and reflection of the light.

Note: Note that fixed cell samples prepared in step 1.5 will be good for couple of weeks and can be used to image at user convenience. Sample or cell preparation outlined in steps 1.6, 1.7, and 1.8 should be prepared when the user is ready to start imaging.

2) Spectral Image Acquisition:

2.1) Turn the microscope system 30 minutes prior to imaging to allow the system warm up and to achieve optimal running conditions.

2.2) Open image acquisition software and load camera and system parameters as detailed in manuscript protocol section 2 for image acquisition. It may be helpful to open a prior saved image and reuse the camera and device settings.

2.3) Place the microscope slide containing fixed expressing HEK293 cells (from step 1.5) on the microscope objective stage.

2.4) Select a field of view with expressing cells using the wide-field fluorescence mode and eyepiece.

2.5) Change to A1 or confocal mode and click the XY button on the A1 plus settings window to acquire one XY plane image (this yields the spectrum of FRET signal containing donor and acceptor signals).

2.6) Save the acquired spectral image.

2.6.1) Click “File” on the top of the acquisition software window.

2.6.2) Click “Save As” under the drop-down list on the file menu.

2.6.3) Click the “folder symbol” in the pop-up window called “Save As Image” to browse and select the folder to save the image in.

2.6.4) Give the image an appropriate filename in the box next to “File name”.

2.6.5) Click save.

2.7) Open the A1 settings window and check the box corresponding to the 488 nm laser (acceptor excitation wavelength) and uncheck the box corresponding to the 405 nm laser line.

2.8) Click OK on the A1 settings window.

2.9) Set the 488 nm laser intensity at 2%.

2.10) Acquire one XY image by clicking the XY button on the A1 plus settings window and save the image as mentioned in steps 2.6.1 – 2.6.2.

Note: This should yield an acceptor signal excited using the acceptor excitation wavelength (i.e., the pure acceptor spectrum).

2.11) Switch the laser line to 514 nm as explained in step 2.7 and set the laser intensity to 100%.

2.12) Click live and expose the sample to 514 nm irradiation until the acceptor signal is completely photobleached.

Note: The time taken for complete photobleaching of acceptor may vary from microscope to microscope depending on the power at the stage, age of the laser and/or type of the microscope system. In our studies, the acceptor fluorophore was completely photobleached (no acceptor signal seen when excited using 488 or 405 nm lasers) in ~ 1.5 hour.

2.13) Switch the laser back to 405 nm and acquire one XY image by clicking the XY button and then save the image as explained in steps 2.6.1 – 2.6.2.

Note: This should yield a donor signal excited using the donor excitation wavelength and in the absence of the acceptor (i.e., the pure donor spectrum). Note that when the acceptor signal is completely photobleached in step 2.12, a pure donor spectral signature is obtained from the same concentration of donor fluorophore as was obtained from the acceptor fluorophore in step 2.10.

2.14) Remove the microscope slide from the stage.

2.15) Place the cell chamber containing single label control for nuclear dye (as prepared in the step 1.6) on the microscope objective stage.

2.16) Open A1 settings menu by clicking the gear symbol on the A1 Plus setting window and check the boxes corresponding to 405 nm and 561 nm laser lines.

2.17) Click "OK".

2.18) Acquire XY image by clicking on "XY" icon on "A1 Plus settings" window (this yields the pure DRAQ5 spectrum).

2.19) Save the image using an appropriate file name as explained in steps 2.6.1 – 2.6.5.

2.20) Place the sample prepared in step 1.8 (cell chamber containing plain coverslip without cells) on the microscope stage.

2.21) Acquire XY image and save the image using an appropriate file name as explained in steps 2.6.1 – 2.6.5. (this yields a non-specific background spectral signatures resulting from coverslip fluorescence (424 nm peak) and from reflection of the light (505 nm peak)).

2.22) Place the cell chamber prepared in step 1.7 (cell chamber containing coverslip with non-expressing cells) on the microscope stage.

2.23) Acquire and save XY image as explained in steps 2.6.1 – 2.6.5 (this yields a spectral image to obtain cell/matrix autofluorescence spectrum).

3) Extract Spectral Information:

3.1) Create a new individual folder corresponding to images saved in steps 2.6, 2.10, 2.13, 2.18, 2.21, and 2.23.

3.2) Export nd2 files into individual tiff files as described in manuscript protocol steps 3.1 (refer to "Table of Materials" for the software used for image acquisition and data exportation).

3.3) Extract donor spectrum: This can be done using several image analysis software platforms. ImageJ software is used in these studies.

3.3.1) Open image analysis platform ("ImageJ" is used in these studies).

3.3.2) In the main menu, select File → Import → Image Sequence.

3.3.3) Browse to the folder containing the exported .tiff image files (exported in step 3.2) for the spectral image that was acquired using 405 nm excitation. This opens an image stack (each slice in the stack represents an emission wavelength of the spectral image).

3.3.4) Draw regions of interest using the rectangular selection tool (or other shape tool if desired).

Note: Make sure that the regions of interest selected contain sufficient signal intensity and that they do not contain oversaturated pixels (for examples, see Figure 3, A and B in the manuscript). Note that Specify Selection tool may also be used to accurately define the size of a rectangular ROI.

3.3.5) In the main ImageJ window select Analyze → Tools → ROI Manager.

3.3.6) Within the ROI Manager, click ADD. This adds the information of the X and Y coordinates of the ROI to the ROI Manager.

3.3.7) Hover to more in the ROI Manager and click Save.

3.3.8) Select a destination folder and save the regions of interest for further use (if needed) or for documentation (recommended).

3.3.9) In the main ImageJ window select Image → Stacks → Plot Z-Axis Profile.

3.3.10) Click "List" on the pop-up window. This displays the set of values in a new window called Plot Values.

3.3.11) Copy the values from this list.

Note that the Y-axis represents the mean intensity value at a given emission wavelength (X-axis).

3.3.12) Open spreadsheet software, such as Microsoft Excel, and paste the intensity values as a column. Save the Excel file with a file name such as "Spectral Library".

3.3.13) Create a heading (name) row that contains "Wavelength (nm)" and the endmember names of the spectral library (in this case in the 1st row enter "Wavelength (nm)", in the 2nd row enter "Turquoise", in the 3rd row "Venus", in the 4th row "DRAQ5", in the 5th row "Background @424nm", in the 6th row "Background @510nm", and in the 7th row "Autofluorescence").

3.3.14) Enter the wavelength information (i.e., 414 – 724 with 10nm intervals excluding wavelength number 564 nm) in the 1st column corresponding to wavelength.

3.3.15) Within the "Plot Values" window on ImageJ, copy the values in the second column and paste these values into the spreadsheet for the column corresponding to Turquoise.

3.4) Extract the acceptor spectrum:

3.4.1) Open the *.tiff image file sequence that was exported in step 3.2 corresponding to the spectral image of the H188 FRET sensor acquired using 488 nm excitation (for the Venus spectrum).

3.4.2) Copy the region(s) of interest that were created and saved in steps 3.3.8 and apply to the Venus image stack. If the ROI manager is closed, open it again and load the saved ROIs (Analyze →Tools→ROI Manager→Open).

3.4.3) Repeat steps 3.3.9 and 3.3.11 and paste the values into the spreadsheet column corresponding to Venus.

Note that these values correspond to the Venus emission spectrum when excited using a 488 nm laser. However, for linear unmixing and further FRET efficiency calculations, it is necessary to correct the Venus spectrum to units that would be obtained as if Venus were excited using the same acquisition settings as those used to measure the Turquoise spectrum (i.e., the 405 nm

laser). To correct the Venus spectrum obtained with 488 nm laser excitation back to similar intensity units as would be expected with 405 nm laser excitation perform the following steps:

3.5) Test the laser linearity of the confocal system using either a laser power meter or a fiber-coupled spectrometer with integrating sphere calibrated to a NIST traceable light source (refer to "List of materials" for the details).

3.5.1) Collect the absolute irradiance of the 405 nm laser line and the 488 nm laser line over a range of illumination intensities (e.g., 0%, 5%, 10%, 20%, 30%, 40%, …, 100%).

3.5.2) Plot the integrated absolute irradiance (units of mW or total photons) detected (Y-axis) at each laser intensity (X-axis) for each laser line. For the laser platform on the Nikon A1R, we have found that the laser response with intensity setting is linear (this should be the case for most laser platforms on most confocal microscopes).

3.5.3) Fit a linear trendline to the data for each laser response and make note of the trendline equation. This equation can be used for comparing laser intensities at any setting (see below).

3.5.4) Using laser trendline equations, calculate total number of photons measured at 2% and at 8% laser intensities of 405 and 488 nm laser lines.

3.5.5) Correct the Venus emission intensity obtained at each wavelength when excited using the 488 nm laser (in step 3.4) to obtain the Venus emission intensity that would be expected if excited using a 405 nm laser using the following equation (Beer-Lambert's Law):

$$I_{Venus_{405\ nm\ @8\%}} = I_{Venus_{488\ nm\ @\ 2\%}} * \left(\frac{A_{Venus\ @405}}{A_{Venus@488}}\right) * \left(\frac{\#of\ Photons_{405\ nm@8\%}}{\#\ of\ Photons_{488\ nm\ @\ 2\%}}\right)$$

where, I is emission intensity (at each emission wavelength) and A is absorbance measured using spectrofluorimeter at specified wavelengths.

Note: We set the 405 nm laser line to 8% laser intensity during image acquisition. However, to avoid oversaturated pixels, we set the 488 nm laser line to 2% intensity for acquiring Venus image. So, when correcting the Venus image from 488 nm to 405 nm, the values of the two laser lines at the two different illumination intensity settings were used by calculating the intensity values from the linear trendlines for each laser.

3.5.6) Create a new column in the excel spread sheet to paste the corrected Venus spectral data.

3.6) Open the sequence corresponding to the DRAQ5 control image, draw regions of interests and extract the spectral information of selected regions by repeating steps 3.3.9 and 3.3.11. Paste the spectral data that corresponds to pure DRAQ5 to the "DRAQ5" column of the spreadsheet created in steps 3.3.12 – 3.3.13.

3.7) Repeat steps 3.3.9 and 3.3.11 to extract spectral data corresponding to two different background spectral signatures: 424 nm (select a region of interest with peak intensity at 424 nm) and 510 nm (select a region of interest with peak intensity at 510 nm). Extract the average

spectrum from each region and paste them in the columns corresponding to “424 nm Background” and “510 nm Background” of the excel sheet created in step 3.3.12.

Note: Two different signal patterns and spectral signatures were observed when imaging the sample blank (plain coverslip). These signatures have been described here as background signatures with a peak intensity of either 424 nm or 510 nm. Both of these signatures may be extracted from the same control image that was acquired using plain coverslip.

3.8) Extract spectral data corresponding to the “autofluorescence” from the image acquired using control cells (from step 2.23) and paste the spectral information in the column corresponding to “Autofluorescence” of the spreadsheet created in step 3.3.12.

3.9) Normalize each spectrum in the spectral library, EXCEPT for the Venus spectrum, to a peak value of unity by dividing each spectrum by the value at the highest intensity wavelength (e.g., peak normalized to a value of one).

3.10) Normalize the Venus spectrum with respect to the peak value of the Turquoise spectrum (Venus and Turquoise spectral data are both normalized to the peak signal intensity of Turquoise).

3.11) Create the spectral library as a MATLAB variable. An example spectral library is provided on the University of South Alabama BioImaging and BioSystems website, under the Resources tab (https://www.southalabama.edu/centers/bioimaging/resources.html)

3.11.1) Open programming software (refer to “List of materials” for the details on programming software used).

3.11.2) Create a new variable called ‘Library’.

3.11.3) Copy and paste the normalized data (step 3.9 and 3.10) into the ‘Library’ variable.

3.11.4) Create a new variable called ‘EndMember_Name’ and enter the names of each endmember in the same order in which the spectral information is pasted into Library file.

3.11.5) Save the Library and EndMember_File together with the filename “Library.mat” or similar that can be easily identified (add a date or experiment number to the file name if desired).

3.12) Open a new variable called ‘Wavelengths’ and enter wavelength numbers corresponding to channels in the spectral image as a signal column.

3.13) Save the wavelength variable as “Wavelengths.mat” or a similar file name and place the file in the same folder in which the library file is saved.